Novel Colorimetric Sensors with Extended Lifetime for Personal Exposure Monitoring

by

Chenwen Lin

A Dissertation Presented in Partial Fulfillment
of the Requirements for the Degree
Doctor of Philosophy

Approved September 2019 by the
Graduate Supervisory Committee:

Nongjian Tao, Chair
Chad Borges
Mark Hayes

ARIZONA STATE UNIVERSITY

December 2019

ABSTRACT

Air pollution has been linked to various health problems but how different air pollutants and exposure levels contribute to those diseases remain largely unknown. Researchers have mainly relied on data from government air monitoring stations to study the health effects of air pollution exposure. The limited information provided by sparse stations has low spatial and temporal resolution, which is not able to represent the actual exposure of individuals. A tool that can accurately monitor personal exposure provides valuable data for epidemiologists to understand the relationship between air pollution and certain diseases. It also allows individuals to be aware of any ambient air quality issues and prevent air pollution exposure. To build such a tool, sensors with features of fast response, small size, long lifetime, high sensitivity, high selectivity, and multi-analyte sensing are of great importance.

In order to meet these requirements, three generations of novel colorimetric sensors have been developed. The first generation is mosaic colorimetric sensors based on tiny sensor blocks and by detecting absorbance change after each air sample injection, the target analyte concentration can be measured. The second generation is a gradient-based colorimetric sensor. Lateral transport of analytes across the colorimetric sensor surface creates a color gradient that shifts along the transport direction over time, and the sensor tracks the gradient shift and converts it into analyte concentration in real-time. The third generation is gradient-based colorimetric arrays fabricated by inkjet-printing method that integrates multiple sensors on a miniaturized sensor chip. Unlike traditional colorimetric sensors, such as detection tubes and optoelectronic nose, that are typically for one-time use,

the presented three generations of colorimetric sensors aim to continuously monitor multiple air pollutants and the sensor lifetime and fabrication methods have been improved over each generation. Ozone, nitrogen dioxide, formaldehyde and carbon monoxide are chosen as analytes of interest. The performance of sensors has been validated in the lab and field tests, proving the capability of the sensors to be used for personal exposure monitoring.

DEDICATION

To my parents and my husband for their endless love and support.

ACKNOWLEDGMENTS

First and foremost, I would like to take the opportunity to thank my advisor Dr. Nongjian Tao, for his generous guidance and unconditional support throughout my graduate studies. He helped me grow as a researcher and trained me to think critically and solve problems independently with great patience. I cannot imagine a better mentor.

I would like to thank Dr. Chad Borges and Dr. Mark Hayes for taking the time to serve on my committee and providing valuable advice in different aspects of my research. It is grateful to have them as my committee members.

I would like to express my gratitude to Dr. Di Wang and Dr. Xiaojun Xian for their guidance and support in my research. Their great help in synthesis, hardware design, and fabrication made my research went smoothly.

Finally, I am thankful to current and previous colleagues I have worked with: Dr. Yue Deng, Dr. Jingjing Yu, Dr. Zijian Du, Mr. Kyle Mallires, Dr. Vishal Tipparaju Dr. Chenbin Liu, Dr. Cheng Chen, Dr. Dangdang Shao, Dr. Yuting Yang, Dr. Francis Tsow, Dr. Devon Bridgeman, Dr. Ashley Quach, Dr. Yixian Wang, Dr. Fenni Zhang, Dr. Wenwen Jing, Dr. Yueqi Li, Ms. Runli Liang, Dr. Shaopeng Wang, Dr. Yan Wang, Dr. Yunze Yang, Dr. Hui Yu and Dr. Xianwei Liu. It has been a great pleasure working with them.

TABLE OF CONTENTS

Page

LIST OF TABLES

Table Page

LIST OF FIGURES

Figure Page

1 INTRODUCTION

The increased level of air pollution is one of the most serious problems in the world. Air pollution has been associated with different health issues, for example, short term exposure to air pollution causes nausea, headaches, and irritation of the upper respiratory tract, whereas long term exposure leads to respiratory diseases, lung cancer and heart diseases. [1-5] Environmental protection agency (EPA) and world health organization (WHO) have set up standards to help regulate air pollution. Table 1 shows the standards for typical air pollutants including ozone (O_3), nitrogen dioxide (NO_2), carbon monoxide (CO) and formaldehyde (HCHO).[6-8] However, the impact of air pollution exposure varies from people to people and even the air pollutant level is under the exposure limit, there may still be adverse health effects. Moreover, it is not clear how different air pollutants and exposure levels contribute to certain diseases.

Traditional air quality monitoring relies on expensive, bulky and complicated instruments installed in fixed government monitoring sites or mobile car monitoring stations. Some of them use passive samplers that required further analysis by gas chromatography (GC) coupled with different detection methods in a lab. [9-11] Researchers have been using data obtained by these traditional methods, but because the level of an air pollutant changes from time to time and place to place, the sparse stations cannot provide data with enough temporal and spatial resolution for correlating individual exposure with symptoms accurately. It is essential to have a tool that can measure accurate personal exposure 24 hours a day. Having such a tool will help epidemiologists to unravel

diseases-exposure relationship. Furthermore, patients who suffered from air pollution-related diseases, such as asthma, can better manage their exposure and prevent an attack.

Table 1.1 Air quality standards for ozone, nitrogen dioxide, carbon monoxide and formaldehyde

	Maximum concentration allowed when averaged over time	
	1 hour	8 hour
Ozone		
WHO		50 ppbV
EPA	120 ppbV	70 ppbV
Nitrogen Dioxide		
WHO	106 ppbV	
EPA	100 ppbV	
Carbon Monoxide		
WHO	26 ppmV	9 ppmV
EPA	35 ppmV	9 ppmV
Formaldehyde		
OSHA		75 ppbV
NOISH		16 ppbV

Sources: World Health Organization(WHO), US Environmental Protection Agency (EPA), European Union (EU), Occupational Safety and Health Administration(OSHA) and National Institute for Occupational Safety and Health (NIOSH)

In order to build a tool for personal exposure monitoring, a sensor with these characteristics is highly preferred: 1) The sensor is sensitive enough to detect trace gases since even air pollutants at ppb or ppm levels by volume may cause health risks. 2) The sensor is selective enough to detect target analytes. Otherwise, it would be difficult to tell which compound in the air contributes to the sensor response. 3) The sensor response is

fast enough to report real-time gas concentration. 4) The sensor size is small considering the application to be regularly used as a personal monitor and not confined to a monitor station5) The sensor can detect target analytes continuously and sensor lifetime is reasonable without frequent replacement. 6) The sensor operation, replacement should be as simple as possible and should not require maintenance by expertise. 7) The cost of the sensor is affordable, which is an important factor for its practical use by people in general. 8) The sensor is expandable to detect multiple analytes simultaneously since there are many gases in the air.

Colorimetry is a well-known sensing principle that is widely used in gas sensing. [12] It detects a color change associated with a specific chemical reaction between an analyte and sensing materials. Colorimetric sensors are cost-effective, selective and user-friendly. However, most colorimetric sensors such as detection tube and electronic noses are typically for one-time use and for qualitative or semi-quantitative analysis only. [13-16] For these reasons, current colorimetric sensors are not suitable for applications that require continuous sensing.

To overcome the drawbacks, this thesis focuses on developing three generations of novel colorimetric sensors aimed for continuous detection for an extended long lifetime. Sensor hardwares utilizing a cost-effective and ubiquitously available light source and detector (complementary metal-oxide-semiconductor (CMOS) imager) have been optimized for sensitive and quantitative detection. Real tests have been done to show the applicability of the developed sensors in personal exposure monitoring, which meet the requirements as mentioned above.

References

[1] Bernstein, J. A.; Alexis, N.; Bacchus, H.; Bernstein, I. L.; Fritz, P.; Horner, E.; Li, N.; Mason, S.; Nel, A.; Oullette, J., The health effects of nonindustrial indoor air pollution. *Journal of Allergy and Clinical Immunology* **2008,** *121* (3), 585-591.

[2] Samet, J. M.; Marbury, M. C.; Spengler, J. D., Health effects and sources of indoor air pollution. Part I. *American Review of Respiratory Disease* **1987,** *136* (6), 1486-1508.

[3] Schwartz, J., Air pollution and hospital admissions for heart disease in eight US counties. *Epidemiology* **1999**, 17-22.

[4] Cohen, A. J., Outdoor air pollution and lung cancer. *Environmental health perspectives* **2000,** *108* (suppl 4), 743-750.

[5] Hwang, J.-S.; Chan, C.-C., Effects of air pollution on daily clinic visits for lower respiratory tract illness. *American journal of epidemiology* **2002,** *155* (1), 1-10.

[6] National Ambient Air Quality Standards. https://www.epa.gov/criteria-air-pollutants/naaqs-table#3.

[7] WHO, Air quality guidelines for Europe. **2000**.

[8] Occupational Safety and Health Standards-Formaldehyde. https://www.osha.gov/pls/oshaweb/owadisp.show_document?p_id=10075&p_table=STANDARDS.

[9] Wennrich, L.; Popp, P.; Hafner, C., Novel integrative passive samplers for the long-term monitoring of semivolatile organic air pollutants. *Journal of Environmental Monitoring* **2002,** *4* (3), 371-376.

[10] Klánová, J.; Kohoutek, J.; Hamplová, L.; Urbanová, P.; Holoubek, I., Passive air sampler as a tool for long-term air pollution monitoring: Part 1. Performance assessment for seasonal and spatial variations. *Environmental Pollution* **2006,** *144* (2), 393-405.

[11] Zhao, B.; Zhang, S.; Zhou, Y.; He, D.; Li, Y.; Ren, M.; Xu, Z.; Fang, J., Characterization and quantification of PAH atmospheric pollution from a large petrochemical complex in Guangzhou: GC–MS/MS analysis. *Microchemical journal* **2015,** *119*, 140-144.

[12] Gilchrist, A.; Nobbs, J., Colorimetry, Theory. In *Encyclopedia of Spectroscopy and Spectrometry*, Lindon, J. C., Ed. Elsevier: Oxford, 1999; pp 337-343.

[13] *Dräger-Tube/CMS Handbook: Handbook for short term measurements in soil, water and air investigations as well as technical gas analysis.* 16th Edition ed.; Dräger Safety AG & Co KGaA: Lübeck, 2011; p 225.

[14] Feng, L.; Musto, C. J.; Kemling, J. W.; Lim, S. H.; Suslick, K. S., A colorimetric sensor array for identification of toxic gases below permissible exposure limits. *Chemical Communications* **2010,** *46* (12), 2037-2039.

[15] Lim, S. H.; Feng, L.; Kemling, J. W.; Musto, C. J.; Suslick, K. S., An optoelectronic nose for the detection of toxic gases. *Nature chemistry* **2009,** *1* (7), 562.

[16] Huang, X.-w.; Zou, X.-b.; Shi, J.-y.; Guo, Y.; Zhao, J.-w.; Zhang, J.; Hao, L., Determination of pork spoilage by colorimetric gas sensor array based on natural pigments. *Food chemistry* **2014,** *145*, 549-554.

2 BACKGROUND

2.1 Air pollution and health risks

Air pollution is a mixture of solid particles and gases, which is the contamination in the air we breathe. It is a major challenge in the world.[17-19] The WHO reported that there is an estimation of 1.8 billion children live in areas where outdoor air pollution is over standard limits and 0.6 million children died from air pollution-related diseases.[7] Children and elderly people are especially vulnerable to adverse health effects from exposure to air pollution.[20-23] Air pollution exposure is responsible for heart diseases, asthma and other respiratory diseases, cancer, adverse pregnancy outcomes (such as preterm birth), and even death.[24-31] Figure 2.1 shows three types of air pollution: criteria pollutants, greenhouse gases and toxic air contaminants and among those, criteria pollutants are the most critical gases that have regional impacts and threatens human health.

O_3 in the upper atmosphere can protect us from ultraviolet radiation. But O_3 at ground level is a well-known respiratory irritant.[32] It is formed in the atmosphere through reactions of nitrogen oxides and volatile organic compounds (VOCs) emitted by vehicles, solvents and industry.[33] Short-term exposure to O_3 causes throat irritation, coughing and chest pain, whereas long-term exposure can lead to decreased lung function, trigger asthma attack and cause chronic obstructive pulmonary disease (COPD).[34-39]

NO_2 are produced primarily by the combustion processes, formed in vehicle engines, and can result in significant inflammation of the airways, development and exacerbations of asthma, bronchitis, as well as lead to a higher risk of heart disease.[39-43]

HCHO is a colorless gas with strong odor. It occurs mostly indoors and emits from adhesives, permanent-press fabrics, paper product coatings and pressed-wood products, such as particleboard, plywood, and fiberboard.[44-47] High-dose exposure of HCHO increases the risk of acute poisoning, while prolonged exposure can lead to chronic toxicity and even cancer.[48-50] Recently, many cases of poisoning, allergy, asthma, pulmonary damage, cancer and death were reported as a result of formaldehyde exposure from polluted indoor air.[51-52]

CO is a well-known silent killer as it is toxic but colorless, odorless, and notoriously difficult to detect. It is generated by the incomplete oxidation during combustion from furnaces, stoves, heaters, and automobiles. Personal exposure of CO causes various symptoms depending on CO exposure duration and concentration. Mild and moderate CO poisoning causes symptoms like the flu, resulting in a headache, fatigue, shortness of breath, nausea, and dizziness. More severe symptoms can be triggered progressively by high level of CO poisoning, including mental confusion, vomiting, loss of muscular coordination, loss of consciousness, and ultimately death. Although there is an increasing awareness of the threat of CO poisoning, reports have shown that unintentional non-fire-related CO poisoning still leads to an estimated 15,000 emergency department visits and approximately 500 deaths annually in the United States alone. [53-54]

Figure 2.1 Types of air pollution and potential health risks.[55]

2.2 Air pollution detection- the gold standard

EPA scientists have developed and evaluated the gold standard method for measuring critical air pollutants accurately and reliably. These methods are called federal reference methods (FRMs) and federal equivalent methods (FEMs).[56] The FRM for O_3

and NO_2 measurements is chemiluminescence, which detects the emission of light resulting from chemical reactions.[57] UV absorption, as a FEM, is also widely used for O_3 monitoring.[58] In addition, gas chromatography and mass spectrometry (GC-MS) is one of the most reliable technologies for gas quantification analysis. GC-MS uses a column to separate different compounds according to different retention times, i.e. the time each compound passed through the column. When the compound leaves the end of the column, the instrument detects and recognizes it. (Fig.2.2).[59] The mass spectrometer first ionizes a compound to generate charged molecules or molecular fragments and measures its mass-to-charge ratio, then it separates them according to their mass-to-charge-ratio. Those separated ions are then detected by a mechanism capable of detecting charged particles. Finally, atoms or molecules can be identified by associating known masses with identified masses. Those separated ions are then detected by a mechanism capable of detecting charged particles. Eventually, atoms or molecules can be identified by associating known masses with identified masses. Although GC-MS techniques exhibit high accuracy in measurement of gas concentration, they are super expensive and bulky to be used for personal exposure monitoring.[60]

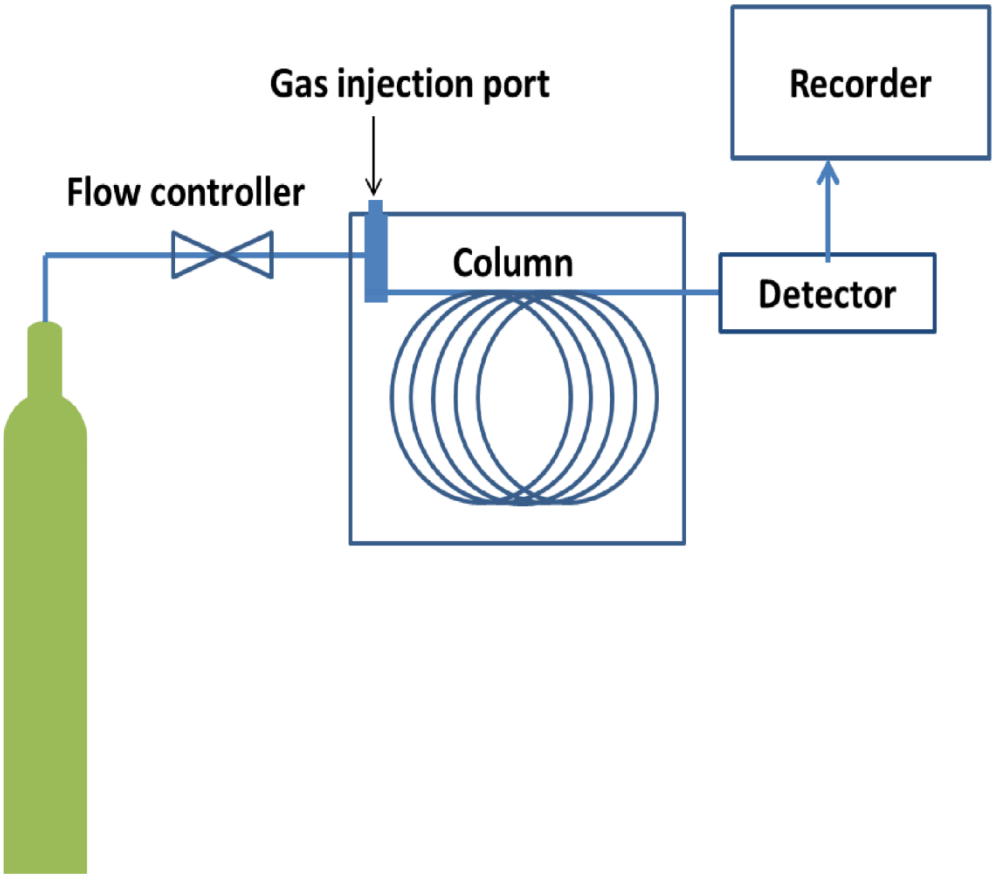

Figure 2.2 Schematic diagram of a gas chromatograph.[59] GC-MS uses a column to separate different compounds according to different retention times and then ionizes and separates charged molecules or molecular fragments by their mass-to-charge-ratio.

2.3 Air pollution detection- state of the art

One of the state-of-the-art sensors for air pollution detection is metal oxide semiconductor (MOS) sensors. As shown in Figure 2.3, when the MOS sensor is in clean air, the oxygen in the air will be adsorbed on a heated semiconductor by capturing free

electrons. When a gas presents, the surface density of adsorbed oxygen changes as it reacts with the gases. The MOS sensor changes resistance because of a change in adsorbed oxygen concentration. This change in conductivity or resistivity can be measure. Research has demonstrated that MOS sensor responds to many kinds of air pollutants such as ozone, NO_2. [61-62] However, selectivity and control of sensor response is a major challenge in this field. MOS sensor usually requires high operation temperature (300-400°C), which increases the power consumption significantly.

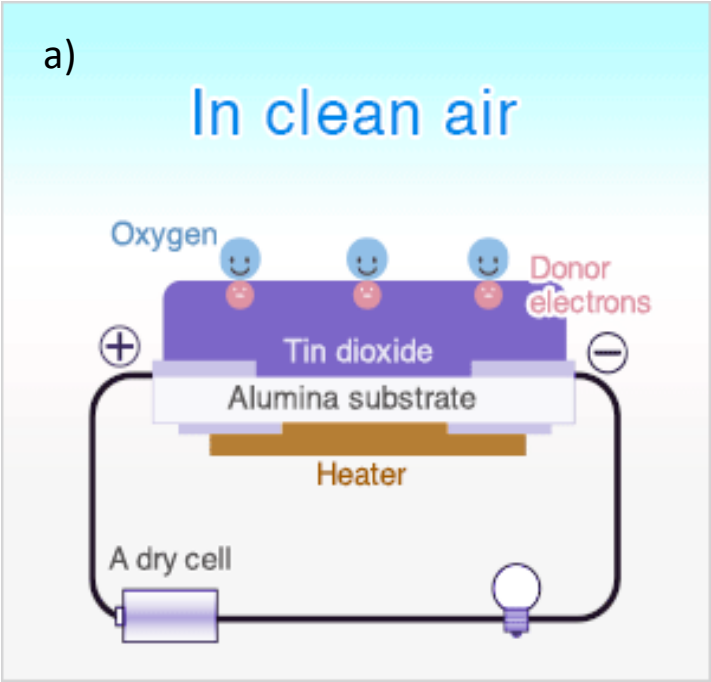

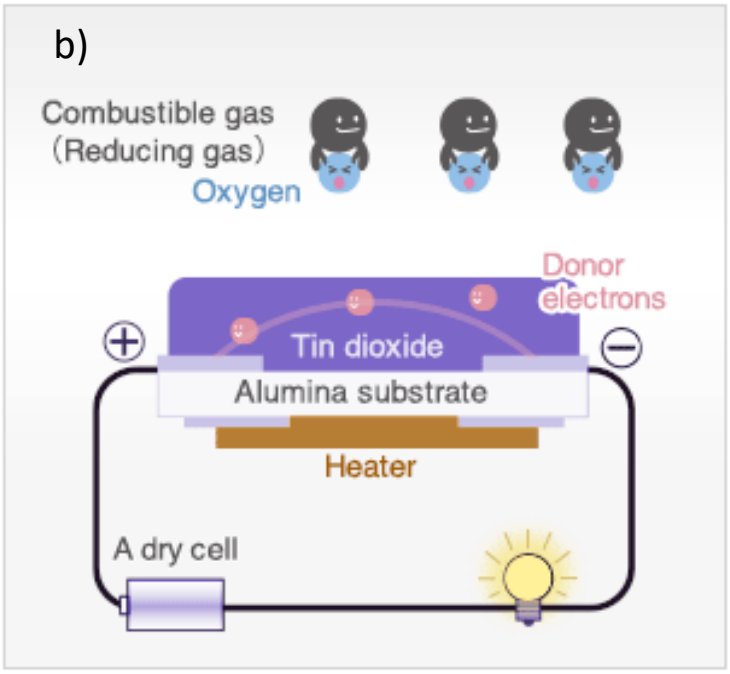

Figure 2.3 Schematic diagram of metal oxide semiconductors. a) The MOS sensor in clean air, b) The MOS sensor in contact with reducing gas resulting in a decrease of sensor resistance. [63]

Another type of sensor is electrochemical sensors. Electrochemical sensors are usually commercialized as convenient portable gas monitors, their target analytes include oxygen, carbon monoxide, hydrogen sulfide and sulfur dioxide. When the gas diffuses into the sensor, through the back of the porous membrane to the working electrode where it is oxidized or reduced. This electrochemical reaction results in an electric current that passes through the external circuit. In addition to measuring, amplifying and performing other signal processing functions, the external circuit maintains the voltage across the sensor between the working and counter electrodes for a two-electrode sensor or between the

working and reference electrodes for a three-electrode cell. At the counter electrode, an equal and opposite reaction occurs, such that if the working electrode is oxidation, then the counter electrode is a reduction.

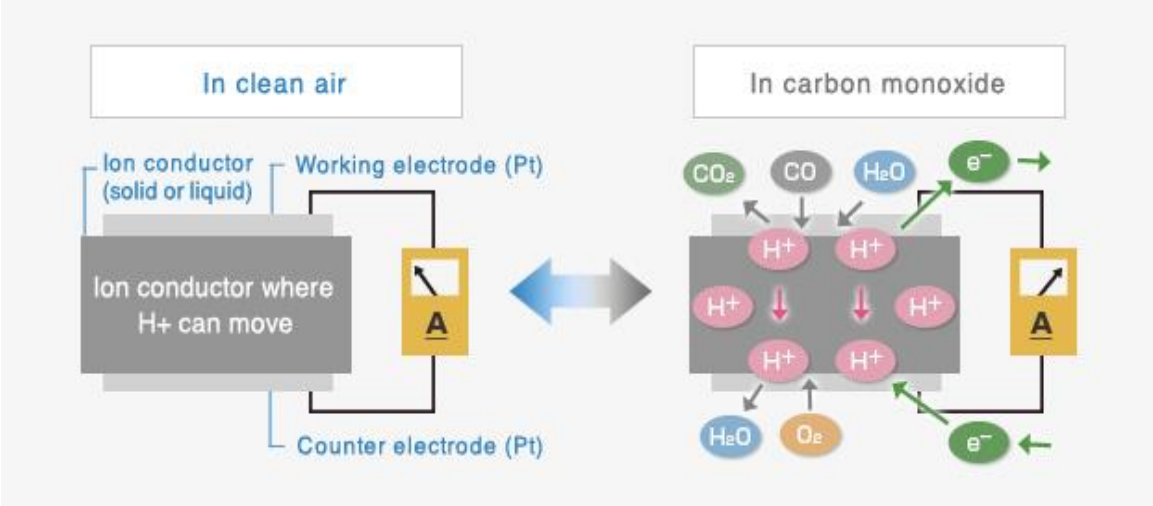

Figure 2.4 Schematic diagram of operating principle of a carbon monoxide electrochemical sensor in clean air and when carbon monoxide gas occurs.[64]

References

[7] WHO, Air quality guidelines for Europe. **2000**.

[17] Brunekreef, B.; Holgate, S. T., Air pollution and health. *The lancet* **2002,** *360* (9341), 1233-1242.

[18] Mills, N. L.; Donaldson, K.; Hadoke, P. W.; Boon, N. A.; MacNee, W.; Cassee, F. R.; Sandström, T.; Blomberg, A.; Newby, D. E., Adverse cardiovascular effects of air pollution. *Nature clinical practice Cardiovascular medicine* **2009,** *6* (1), 36-44.

[19] Saxon, A.; Diaz-Sanchez, D., Air pollution and allergy: you are what you breathe. *Nature immunology* **2005,** *6* (3), 223-226.

[20] Smith, K. R.; Samet, J. M.; Romieu, I.; Bruce, N., Indoor air pollution in developing countries and acute lower respiratory infections in children. *Thorax* **2000,** *55* (6), 518-532.

[21] Morris, R. D.; Naumova, E. N.; Munasinghe, R. L., Ambient air pollution and hospitalization for congestive heart failure among elderly people in seven large US cities. *American journal of public health* **1995,** *85* (10), 1361-1365.

[22] Simoni, M.; Jaakkola, M.; Carrozzi, L.; Baldacci, S.; Di Pede, F.; Viegi, G., Indoor air pollution and respiratory health in the elderly. *European Respiratory Journal* **2003,** *21* (40 suppl), 15s-20s.

[23] Kim, J. J., Ambient air pollution: health hazards to children. *Pediatrics* **2004,** *114* (6), 1699-1707.

[24] Ruckerl, R.; Ibald-Mulli, A.; Koenig, W.; Schneider, A.; Woelke, G.; Cyrys, J.; Heinrich, J.; Marder, V.; Frampton, M.; Wichmann, H. E., Air pollution and markers of inflammation and coagulation in patients with coronary heart disease. *American journal of respiratory and critical care medicine* **2006,** *173* (4), 432-441.

[25] Jerrett , M.; Burnett , R. T.; Pope , C. A. I.; Ito , K.; Thurston , G.; Krewski , D.; Shi , Y.; Calle , E.; Thun , M., Long-Term Ozone Exposure and Mortality. *New England Journal of Medicine* **2009,** *360* (11), 1085-1095.

[26] Guarnieri, M.; Balmes, J. R., Outdoor air pollution and asthma. *The lancet* **2014,** *383* (9928), 1581-1592.

[27] Lelieveld, J.; Evans, J. S.; Fnais, M.; Giannadaki, D.; Pozzer, A., The contribution of outdoor air pollution sources to premature mortality on a global scale. *Nature* **2015,** *525* (7569), 367-371.

[28] Brauer, M.; Hoek, G.; Smit, H.; De Jongste, J.; Gerritsen, J.; Postma, D. S.; Kerkhof, M.; Brunekreef, B., Air pollution and development of asthma, allergy and infections in a birth cohort. *European Respiratory Journal* **2007,** *29* (5), 879-888.

[29] Stieb, D. M.; Chen, L.; Eshoul, M.; Judek, S., Ambient air pollution, birth weight and preterm birth: a systematic review and meta-analysis. *Environmental research* **2012,** *117*, 100-111.

[30] Wilson, E., EPIDEMIOLOGY Long-term exposure to ozone increases risk of death. *Chemical & Engineering News Archive* **2009,** *87* (11), 9.

[31] Pope III, C. A.; Burnett, R. T.; Thun, M. J.; Calle, E. E.; Krewski, D.; Ito, K.; Thurston, G. D., Lung cancer, cardiopulmonary mortality, and long-term exposure to fine particulate air pollution. *Jama* **2002,** *287* (9), 1132-1141.

[32] Patocka, J.; Kuca, K., Irritant compounds: respiratory irritant gases. *Milit Med Sci Lett* **2014,** *83* (2), 73-82.

[33] Torres-Jardon, R.; Keener, T. C., Evaluation of ozone-nitrogen oxides-volatile organic compound sensitivity of Cincinnati, Ohio. *Journal of the Air & Waste Management Association* **2006,** *56* (3), 322-333.

[34] Shah, A. S.; Lee, K. K.; McAllister, D. A.; Hunter, A.; Nair, H.; Whiteley, W.; Langrish, J. P.; Newby, D. E.; Mills, N. L., Short term exposure to air pollution and stroke: systematic review and meta-analysis. *bmj* **2015,** *350*, h1295.

[35] Lin, S.; Liu, X.; Le, L. H.; Hwang, S.-A., Chronic exposure to ambient ozone and asthma hospital admissions among children. *Environmental health perspectives* **2008,** *116* (12), 1725-1730.

[36] McConnell, R.; Berhane, K.; Gilliland, F.; London, S. J.; Islam, T.; Gauderman, W. J.; Avol, E.; Margolis, H. G.; Peters, J. M., Asthma in exercising children exposed to ozone: a cohort study. *The lancet* **2002,** *359* (9304), 386-391.

[37] Khaniabadi, Y. O.; Hopke, P. K.; Goudarzi, G.; Daryanoosh, S. M.; Jourvand, M.; Basiri, H., Cardiopulmonary mortality and COPD attributed to ambient ozone. *Environmental research* **2017,** *152*, 336-341.

[38] Sunyer, J.; Jarvis, D.; Gotschi, T.; Garcia-Esteban, R.; Jacquemin, B.; Aguilera, I.; Ackerman, U.; de Marco, R.; Forsberg, B.; Gislason, T., Chronic bronchitis and urban air pollution in an international study. *Occupational and environmental medicine* **2006,** *63* (12), 836-843.

[39] Latza, U.; Gerdes, S.; Baur, X., Effects of nitrogen dioxide on human health: systematic review of experimental and epidemiological studies conducted

between 2002 and 2006. *International journal of hygiene and environmental health* **2009,** *212* (3), 271-287.

[40] BLOMBERG, A.; Krishna, M. T.; Bocchino, V.; Biscione, G. L.; Shute, J. K.; Kelly, F. J.; Frew, A. J.; Holgate, S. T.; Sandstrom, T., The inflammatory effects of 2 ppm NO_2 on the airways of healthy subjects. *American journal of respiratory and critical care medicine* **1997,** *156* (2), 418-424.

[41] Barck, C.; Sandström, T.; Lundahl, J.; Hallden, G.; Svartengren, M.; Strand, V.; Rak, S.; Bylin, G., Ambient level of NO_2 augments the inflammatory response to inhaled allergen in asthmatics. *Respiratory medicine* **2002,** *96* (11), 907-917.

[42] Chauhan, A.; Inskip, H. M.; Linaker, C. H.; Smith, S.; Schreiber, J.; Johnston, S. L.; Holgate, S. T., Personal exposure to nitrogen dioxide (NO_2) and the severity of virus-induced asthma in children. *The lancet* **2003,** *361* (9373), 1939-1944.

[43] PERSHAGEN, G.; Rylander, E.; Norberg, S.; Eriksson, M.; Nordvall, S. L., Air pollution involving nitrogen dioxide exposure and wheezing bronchitis in children. *International journal of epidemiology* **1995,** *24* (6), 1147-1153.

[44] MEYER, B.; HERMANNS, K., Formaldehyde release from pressed wood products. ACS Publications: 1985.

[45] Kelly, T. J.; Smith, D. L.; Satola, J., Emission rates of formaldehyde from materials and consumer products found in California homes. *Environmental Science & Technology* **1999,** *33* (1), 81-88.

[46] Fowler, J. F.; Skinner, S. M.; Belsito, D. V., Allergic contact dermatitis from formaldehyde resins in permanent press clothing: an underdiagnosed cause of generalized dermatitis. *Journal of the American Academy of Dermatology* **1992,** *27* (6), 962-968.

[47] Conner, A. H., Urea-formaldehyde adhesive resins. *Polymeric materials encyclopedia* **1996,** *11*, 8496-8501.

[48] Kim, K.-H.; Jahan, S. A.; Lee, J.-T., Exposure to formaldehyde and its potential human health hazards. *Journal of Environmental Science and Health, Part C* **2011,** *29* (4), 277-299.

[49] Krzyzanowski, M.; Quackenboss, J. J.; Lebowitz, M. D., Chronic respiratory effects of indoor formaldehyde exposure. *Environmental research* **1990,** *52* (2), 117-125.

[50] Bosetti, C.; McLaughlin, J.; Tarone, R.; Pira, E.; La Vecchia, C., Formaldehyde and cancer risk: a quantitative review of cohort studies through 2006. *Annals of Oncology* **2008,** *19* (1), 29-43.

[51] McGwin, G.; Lienert, J.; Kennedy, J. I., Formaldehyde Exposure and Asthma in Children: A Systematic Review. *Environmental health perspectives* **2010,** *118* (3), 313-317.

[52] Blair, A.; Saracci, R.; Stewart, P. A.; Hayes, R. B.; Shy, C., Epidemiologic evidence on the relationship between formaldehyde exposure and cancer. *Scandinavian Journal of Work, Environment & Health* **1990,** *16* (6), 381-393.

[53] Rajiah, K.; Mathew, E. M., Clinical manifestation, effects, diagnosis, monitoring of carbon monoxide poisoning and toxicity. *Afr. J. Pharm. Pharmacol.* **2011,** *5* (2), 259-63.

[54] Raub, J. A.; Mathieu-Nolf, M.; Hampson, N. B.; Thom, S. R., Carbon monoxide poisoning—a public health perspective. *Toxicology* **2000,** *145* (1), 1-14.

[55] Types of air pollution. https://cceeb.org/resources/air-quality-101/#toxic-air-contaminants.

[56] Sampling Methods for Criteria Pollutants. https://aqs.epa.gov/aqsweb/documents/codetables/methods_criteria.html.

[57] Toby, S., Chemiluminescence in the reactions of ozone. *Chemical Reviews* **1984,** *84* (3), 277-285.

[58] Andersen, P. C.; Williford, C. J.; Birks, J. W., Miniature Personal Ozone Monitor Based on UV Absorbance. *Analytical Chemistry* **2010,** *82* (19), 7924-7928.

[59] Zhao, D. A Novel Handheld Real-time Carbon Dioxide Analyzer for Health and Environmental Applications Arizona State University, 2014.

[60] Badjagbo, K.; Sauvé, S.; Moore, S., Real-time continuous monitoring methods for airborne VOCs. *TrAC Trends in Analytical Chemistry* **2007,** *26* (9), 931-940.

[61] Cao, T.; Thompson, J. E., Personal monitoring of ozone exposure: A fully portable device for under $150 USD cost. *Sensors and Actuators B: Chemical* **2016,** *224*, 936-943.

[62] Shafiei, M.; Kalantar-Zadeh, K.; Wlodarski, W.; Comini, E.; Ferroni, M.; Sberveglieri, G.; Kaciulis, S.; Pandolfi, L., Hydrogen gas sensing performance of Pt/SnO_2 nanowires/SiC MOS devices. *Int. J. Smart Sens. Intell. Syst* **2008,** *1* (3), 771.

[63] MOS type sensors operating principle. http://www.figarosensor.com/technicalinfo/principle/mos-type.html.

[64] Electrochemical type sensors operating principle. http://www.figarosensor.com/technicalinfo/principle/electrochemical-type.html.

3 MOSAIC COLORIMETRIC SENSORS FOR MONITORING MULTI-ANALYTE IN AIR

3.1 Introduction

Air quality has a major impact on our health. Monitoring air quality helps protect people from exposure to harmful gases at home and in the workplace, reduce health risks of millions of patients who suffer from chronic respiratory diseases, and minimize occupational safety threats for workers.[65] It is also important for exposure-diseases relationship study, identification of sources of pollutants, warning of environmental disease triggers, and development of air quality management plan. Besides the stationary monitoring, a wearable sensor for personal exposure monitoring has drawn more and more attention since people engage in activities in different places, e.g. sleeping in the room, traveling in the car, eating in the cafeteria, working in the office, or exercising in the gym.[66-68] Furthermore, as for the needs of efficient air quality monitoring, a highly integrated device, which can monitor multiple pollutants of interests continuously and simultaneously is highly preferred.

While recent advances in sensor technologies are impressive, and some, including electrochemical sensors, colorimetric sensors, metal oxide gas sensors, and UV absorption detectors, are commercially available, but they all suffered from their own limitations. Electrochemical sensors are often interfered by pressure changes and require periodic calibration for an accurate reading, which add a burden to the users. MOS sensors have low selectivity and require high operation temperature (usually from 200 ^{o}C to 500 ^{o}C) with high power consumption.[69-70] Colorimetric sensors detect the color change

induced by a specific chemical reaction between the target analyte and the sensing probe. It has been of interests recently for its high sensitivity, high selectivity, and simplicity. However, most colorimetric sensors, such as detection tubes and pH papers, can only be used for one time, which is not suitable for applications that require continuous sensing.

The mosaic colorimetric sensor presented in this chapter provides an integrated solution for reaching the goal of personal exposure monitoring. The sensor has the following innovations. 1) A porous material is used as a substrate to increase the analyte capture efficiency thus increase the sensor sensitivity. 2) A finely tuned recipe of sensing probes enables high selectivity of each sensor. 3) An active built-in sample delivery system is used to deliver the gas into the detection chamber at a constant flow rate to accelerate mass transport and decrease the response time. The pump can also be programmed to have an adaptive sampling time to ensure the sensitivity and save sensor lifetime.4) A low-cost CMOS imager based optical detection system to allow quantitative detection of gas analytes. All these innovations attribute the novel mosaic colorimetric sensing platform the capability for fast and continuous gas monitoring with a response time of less than 20 seconds. There are other important features that make the mosaic colorimetric sensor unique and attractive. First, an ultralow detection limit of each sensor not only give an alarm at the time when air pollution level exceeds standard limits, but also inform people ahead of time when certain air pollutant exists in the ambient air. Second, the sensor chip is expandable and configurable. By mix and matching different sensor blocks on the sensor chip, multiple gaseous pollutants can be detected for different applications. And third, the

as-prepared sensor chip will be pre-calibrated during production, which avoids putting the calibration burden on the users.

3.2 Detection principle and setup

The chemical reaction happens rapidly when the gas sample is introduced into the reaction chamber.

The detection principle used here was based on a colorimetric change of chemical probe on exposure to target analytes. The detection of color change on the sensing probes is enabled by a sensing platform that consisted of a CMOS imager as an optical detector. The CMOS imager was controlled by a Matlab program developed in the Center for Bioelectronics and Biosensors at the Biodesign Institute. The sensing chamber was made by CNC milling (MAXNC-10) using Acetron, which had gas inlet and outlet, and a sensor slot that can position and align the sensor chip with the optical detection system. A white LED (LEDtronics Inc.) was connected to a LED driver (CL520N3-G-ND) for stable illumination for the sensing chamber. The active sample delivery system was assembled by connecting an air pump (Parker, T3EP-1ST-05-3FFP-b) via a Teflon® tubing, and the flow rate of which was maintained at 1L/min. The CMOS imager captured intensity of each sensor element at a frame rate of 5 frames per second. A blank sensor element, which is a sensor substrate without the coating of sensing probe, was used as a reference to correct other optical factors except for actual sensor signal, including light source change, scattering or noise in the detection system (Figure 3.1). The logarithmic ratio between the sensing and the reference elements was evaluated as the output signal. This signal

corresponded to absorbance change due to the reaction and was directly proportional to the concentration of the analyte.

$$Absorbance = -log\left(\frac{I}{I_0}\right) = -log\left(\frac{I_{sensing}}{I_{reference}}\right) \quad (1)$$

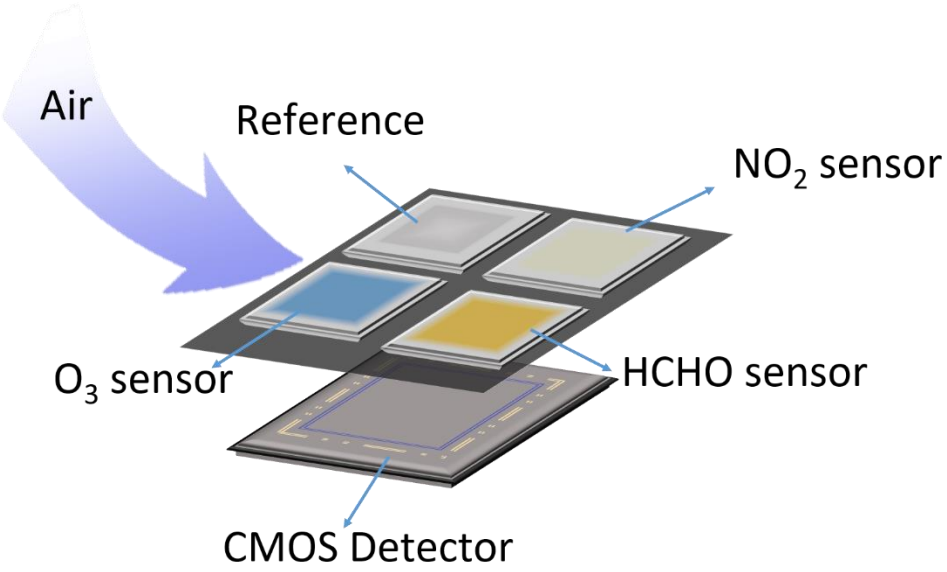

Figure 3.1 Schematic of the sensing setup. The sample gas is delivered at 1 L/min from the Tedlar® air bag to the sensing channel where the reference chip (gray), NO_2 sensor chip (light yellow), O_3 sensor chip (blue) and CO sensor chip (yellow) are located. The white LED illuminates the sensor chip and the transmission light is detected by the CMOS imager.

Figure 3.2 (a) shows the intensity value captured by the imager from the two elements. The chamber was purged with clean air for the first minute. In this duration, the intensity was nearly constant. Note that baseline subtraction will be performed if there is a

slight drift due to the optical system. For the next 20 seconds, the gas sample, CO in this case, was delivered by a pump, which resulted in a linear decrease in the intensity on the sensing element (black curve) due to color development. The reference element (red curve) was not affected by the introduction of the sample. The system was again purged for the next minute. In this duration, the color development stopped, and both sensing and reference elements went back to a constant intensity.

The intensity data was transformed to change in absorbance as shown in Figure 3.2 (b) using equation (1). The absorbance change increased linearly with time. The sensitivity of detection could be optimized by adjusting the sample injection time.

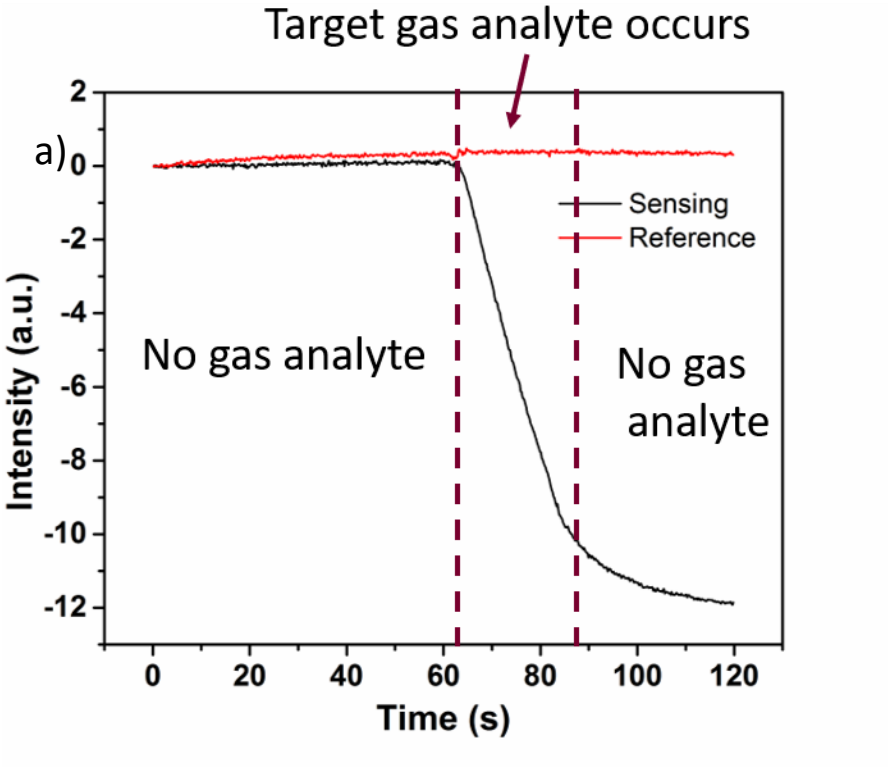

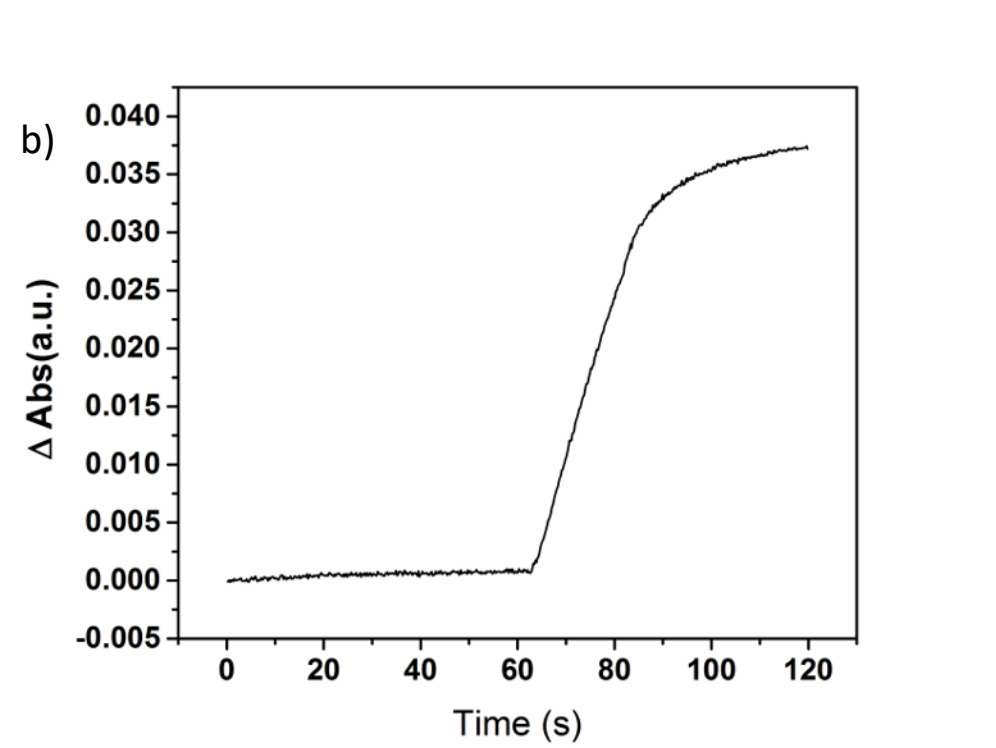

Figure 3.2 (a) Transmitted intensity of light obtained by the CMOS imager from the reference and sensing elements during a test. (b)Absorbance of sensor during a test converted from intensity data

3.3 Experimental

3.3.1 Reagents and sensor preparation

N, N-Diethyl-p-phenylenediamine(DMPPDA), glycerol, hydroxylamine sulfate, thymol blue, methanol, indigo carmine, citric acid were purchased from Sigma-Aldrich, lnc. Potassium disulfitopalladate (II) ($K_2Pd(SO_3)_2$) was purchased from Alfa Aesar. Ultra-pure water (18MΩ) was produced by an ELGA Purelab Ultra RO system. Silica gel substrates were purchased from Sorbent Technologies (Silica G TLC Plates, Polyester

Backed, 20×20 cm, 250 μm thickness, 60 Å mean pore diameter of silica gel, pore volume: ~ 0.75 ml/g, specific surface area: ~ 500 m^2/g). The substrate was cut into 5×5 mm pieces by laser cutter and wash with DI water and ethanol for three times, respectively.

The sensors chips were prepared by immobilizing the sensing element that reacts with specific target analyte selectively on the porous silica gel substrate.

NO_2 sensor: The solution of the sensing element was prepared by dissolving 400 mg of DMPPDA in 4 mL of DI water with 0.5 ml glycerol. The sensor substrates were immersed in the solution and shaken slowly for 1 hour to make uniform coating, followed by overnight vacuum drying under room temperature.

O_3 sensor: The solution of the sensing element was prepared by 9 mg indigo carmine and 700 mg citric acid in a solvent mixture containing 4 mL of DI water with 0.5 ml glycerol. The sensor substrates were immersed in the solution and shaken slowly for 1 hour to make uniform coating, followed by overnight vacuum drying under room temperature.

HCHO sensor: The solution of the sensing element was prepared by dissolving hydroxylamine sulfate (10 mg/ml) and thymol blue (0.2 mg/ml) in a solvent mixture containing methanol, water, and glycerol (volume ration of 6.5:3:0.5). The pH of the solution was adjusted to 5.5 with NaOH solution (5M). The sensor substrates were immersed in the solution and shaken slowly for 1 hour to make uniform coating, followed by overnight vacuum drying under room temperature.

CO sensor: The solution of the sensing element was prepared by dissolving 80 mg of $K_2Pd(SO_3)_2$ in 10 mL of hot DI water. The silica paper was cut into 5×5 mm pieces by

laser cutter and wash with DI water and ethanol for three times, respectively. The 30 μL of $K_2Pd(SO_3)_2$ solution was then drop-casted onto the 5×5 mm silica gel substrate and vacuum dried for 1 hour. The drop-casting process was repeated 4 times to achieve a better sensitivity of the as-prepared CO sensor chip.

3.3.2 Standard gas samples

O_3 samples were generated by an O_3 generator (UVP Corp.) using UV radiation. The actual concentration of each O_3 sample was confirmed by an O_3 analyzer (2B Technologies, Inc.).

Standard CO gas (1000 ppm, balanced with nitrogen) was purchased from Cross company. Standard NO_2 gas (50 ppm in nitrogen) and standard HCHO gas (50 ppm in nitrogen) purchased from Praxair Inc. The various concentrations of gas samples were prepared in 4 L Tedlar® bags (Custom Sensor Solutions Inc.) by dilution with clean air (Praxair Certified Breath Air).

3.3.3 Chemical reactions

O_3 detection is based on the chemical reaction of O_3 with indigo carmine, which is blue at pH<11.4. The reaction product is light yellow isatin sulfonic acid.

NO_2 detection is based on the chemical reaction of NO_2 with N,N-dimethyl-p-phenylenediamine. The reaction product is pink, and the structure of the azo compound is as shown in Figure 3.3.

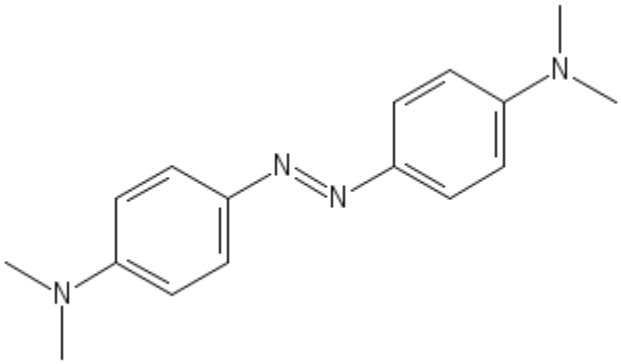

Figure 3.3 Chemical structure of NO_2 reaction product.

HCHO detection is based on the chemical reaction of HCHO with hydroxylamine. The reaction generates protons that changes the pH on the sensor substrate resulting in color change of thymol blue from yellow to red.

CO detection is based on a selective chemical reaction between CO molecules and the sensing elements on the porous substrate:

$$CO + K_2Pd(SO_3)_2 \rightarrow Pd + CO_2 + SO_2 + K_2SO_3 \quad (2)$$

The palladium salts are commonly used in these products as the catalyst for CO oxidation and the molybdenum compounds are used as color indicators. Instead of using palladium salts as a catalyst, which involves in both oxidation (sensing) and reduction (recovery) processes, the CO sensor use the palladium salts as a reactant only for sensing

3.3.4 Calibration curves

The air pump was connected to a mechanical three-way valve for switching between dry clean air and CO sample gas. The gases were stored in Tedlar® bags and delivered to the sensing chamber at a flow rate of 1L/min. A 60s purging of dry clean air to the system was used to establish a stable baseline, and then sample gas at a particular concentration was injected into the system for 20s. The target analyte reacted with the sensing probes on the sensor chip during the sampling period, resulting in a color change, which can be detected by the optical system mounted on the sensing chamber. The schematic diagram of the sensing platform is shown in Fig 3.1. When running the test, the sensor cartridge was assembled in the detection chamber, and the optical detection module continuously recorded the absorbance ($-\log(I_{sensing}/I_{reference})$) change as a function of time during the entire cycle of test. The slope of the optical absorbance curve difference between the sensing and purging periods was calculated, which was correlated with the concentration of target analyte in the gas sample. Figure 3.4 shows the calibration curve of

four target analytes: O_3, NO_2, HCHO and CO. The results all show linear relationship between target analyte concentrations and sensor responses.

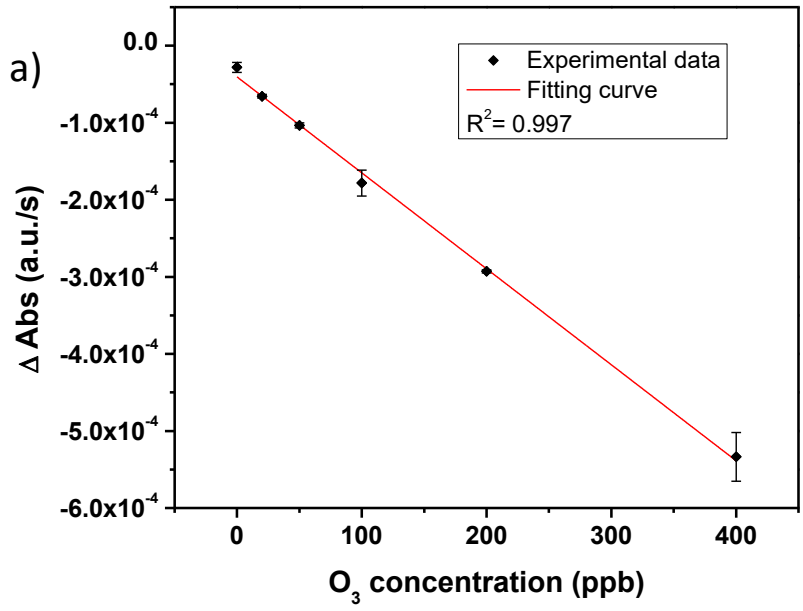

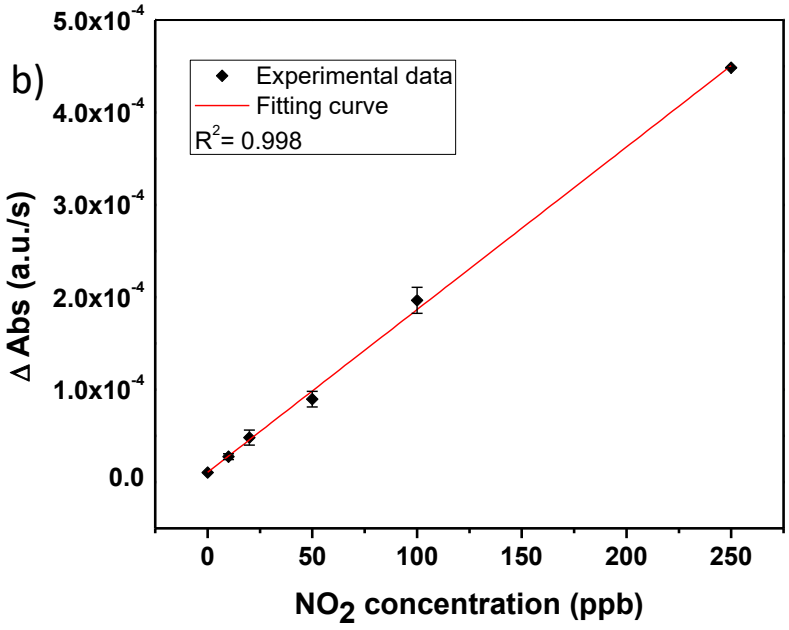

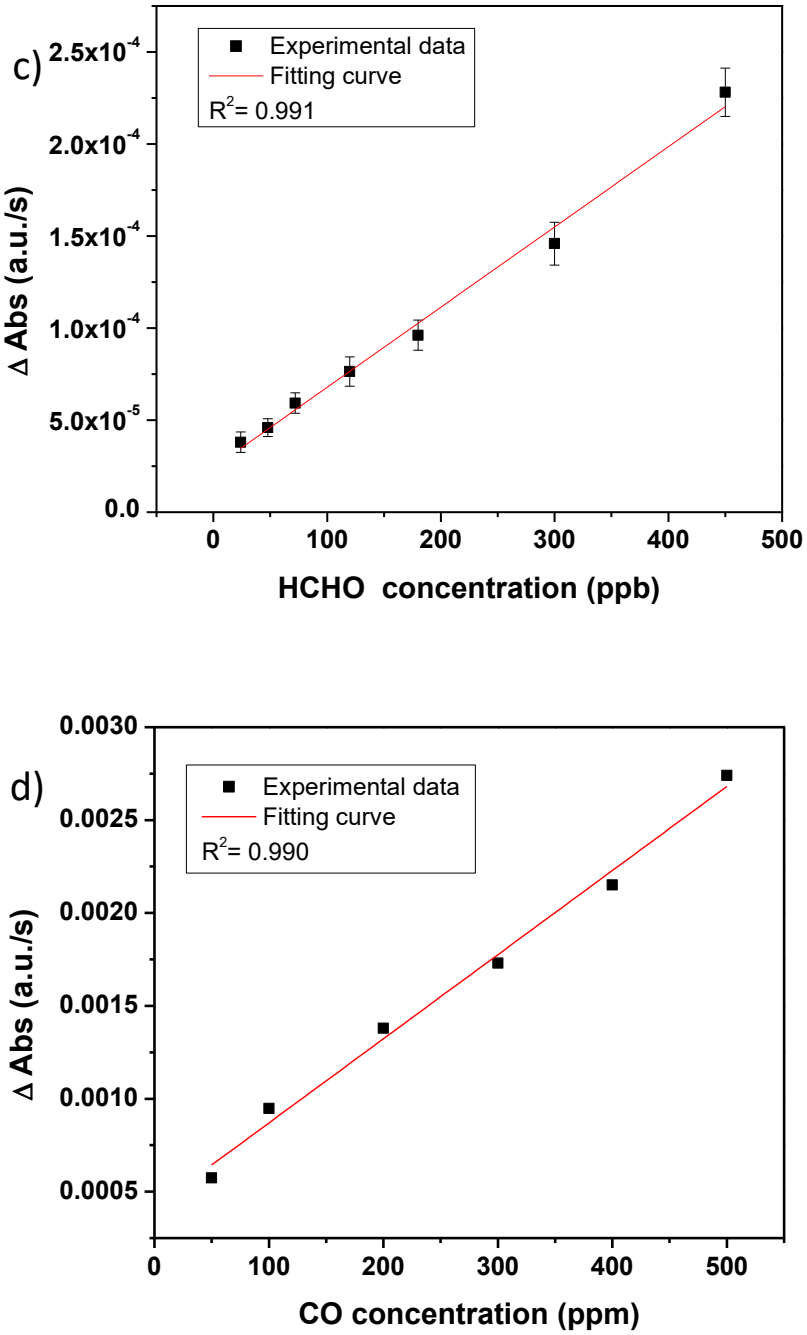

Figure 3.4 Calibration curve of O_3, NO_2, HCHO and CO sensors.

3.4 Results and Discussion

3.4.1 Sensitivity and dynamic range

To achieve the goal of continuous monitoring, the chemical reaction between the analyte and the sensing probe should be fast enough to achieve a fast response time. Here we take CO sensor as an example to demonstrate the sensor performance. The response curves of the sensor to different concentrations of CO have been investigated to evaluate the reaction kinetics of this gas-solid phase reaction. According to Fig. 3.5(a) and Fig. 3.4 (d), the absorbance signal changes spontaneously when the CO gas is injected into the detection chamber, regardless of the CO concentrations in the range of 0 ppm to 500 ppm. It should be noticed that the slope of the absorbance change, which is the absorbance change before and after the injection of CO divided by the corresponding exposure time (Δ Abs=Absorbance change/time, unit: a.u./s), increases with the CO concentrations in the gas samples. And further data analysis shows that these slope values have a good linear relationship with CO concentration. In the lower CO concentration range (0 ppm to 10 ppm) the sensor has higher sensitivity of $(1.7879 \pm 0.152) \times 10^{-5}$ a.u./s·ppm while in the higher CO concentration range, the sensor shows a relative lower sensitivity of $(4.202 \pm 0.252) \times 10^{-6}$ a.u./s·ppm, as plotted in Fig. 3.2 (b) and Fig. 3.2 (d). This linear sensing behavior can be explained according to the model we described in the previous work. Briefly, when the active sites of the sensing elements on the substrate are excessive, the reaction rate depends on the concentration of the analyte in the gas phase.

$$R = K \cdot C_{CO} \tag{2}$$

According to equation (2), where K is a constant that related to surface adsorption and C_{CO} is the concentration of CO, the CO concentration will be proportional to the absorbance slope since the reaction rate (R) can be represented by the slope of the optical absorbance – time plot, which is consistent with the experimental results. We hypothesized the different adsorption and reaction behaviors in the lower and higher CO concentration ranges may contribute to the discontinuity of linear sensor response at 10 ppm. Under low concentration, CO molecules are mainly adsorbed and reacted with sensing elements on the top surface of the substrate, while under high concentration, CO molecules can further diffuse into the porous substrate and react with sensing elements deep inside. It should be mentioned that conventional colorimetric CO sensor cannot reach a detection limit bellow 15 ppm, while our CO sensor can easily discriminate different concentrations of CO bellow 10 ppm with a detection limit of 1 ppm, as shown in Fig. 3.2 (c) and (d). The above sensitivity and detection limit were achieved under the sampling condition of 20 s injection

time and 1L/min flow rate. If needed, these specs can be further improved by applying a longer sampling time or higher flow rate.

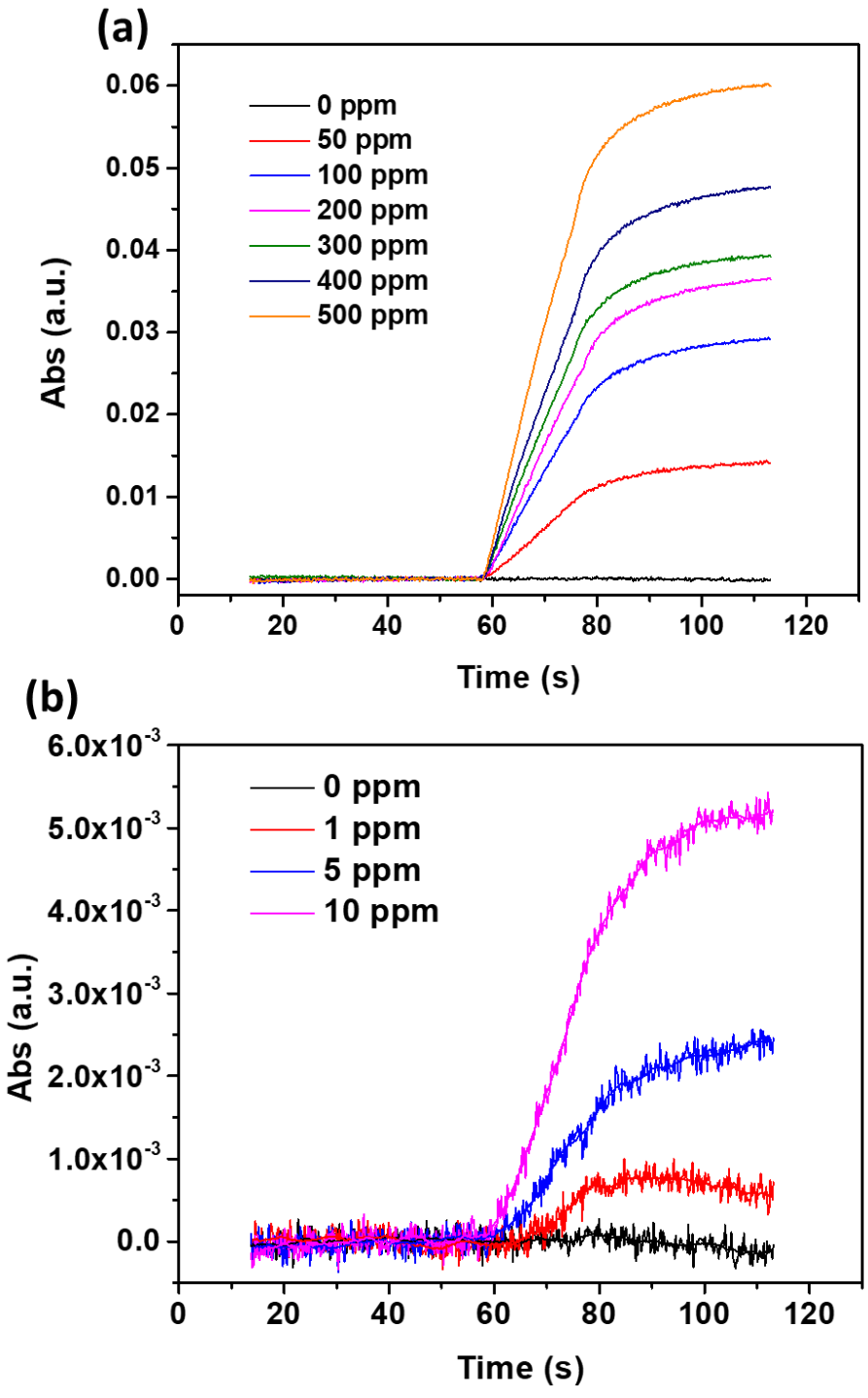

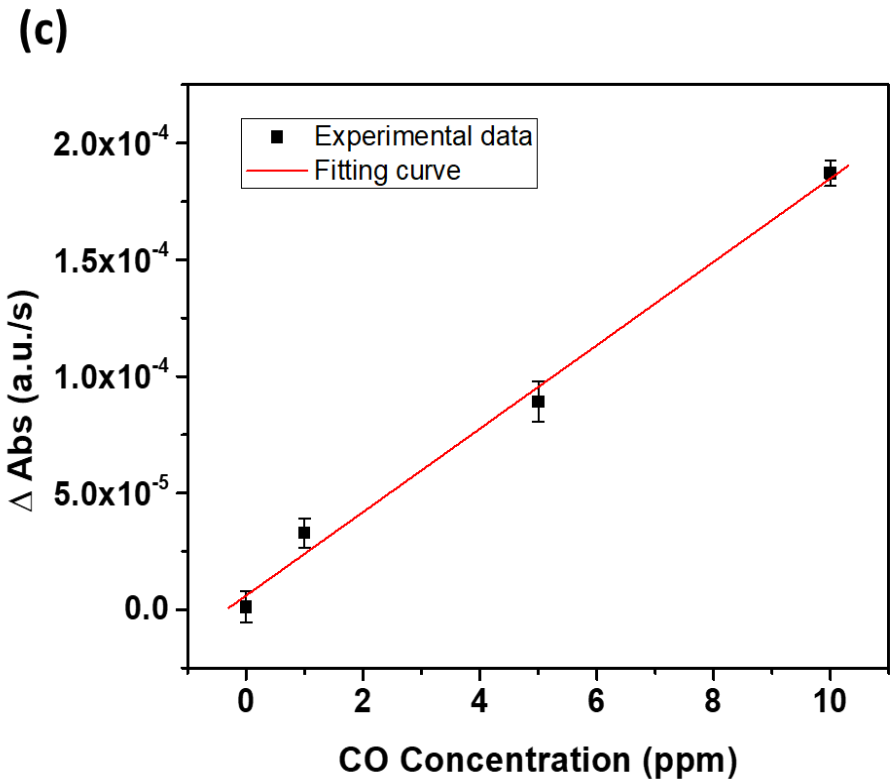

Figure 3.5 (a) The optical responses of the CO sensor to different concentrations of dry CO gas samples. (b) The optical responses of the CO sensor to lower concentrations of dry CO gas samples. (c) Calibration of sensor response to CO.

3.4.2 Sensor response time

Due to the unique features of colorimetric sensors, the sensor response time is related to the time period that the sensor reacts with the target analyte of certain concentration and the color change or absorbance change reachs the detection limit of the sensing platform. The higher the target analye concentration, the shorter the response time.

In this case, the sensor response is defined as 15 seconds in order to detect CO concentration as low as 1 ppm.

3.4.3 Sensor selectivity

The beauty of the colorimetric chemical sensor is that high selectivity can be achieved by applying chemical reactions that are specific to the targeting analyte. This feature differentiates it from other sensing approaches, such as electrochemical sensing, metal oxide sensing, and infrared absorption sensing. Due to the unique reaction between the target analyte and sensing probes, the sensing probes coated on the substrate is very selective to CO while immune to other common interferents in the ambient air. Cross sensitivity test has been performed among O_3, NO_2 and CO sensors and in addition, the following gases at their typical concentration found in the ambient air have been tested on each sensor: O_2, SO_2, NO and ammonia. None of them shows a considerable response, with the signal fluctuations less than 5% of the signal (Fig. 3.6). This high selectivity can avoid the need for scrubbers to remove the potential interferents as in conventional sensor devices in order to achieve acceptable accuracy.

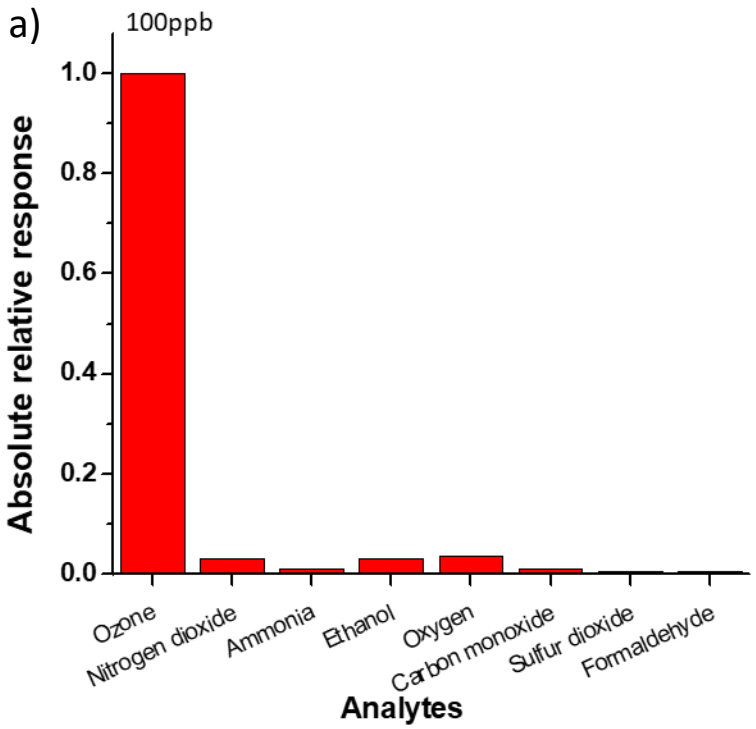
a)
100ppb
Absolute relative response
1.0
0.8
0.6
0.4
0.2
0.0
Ozone
Nitrogen dioxide
Ammonia
Ethanol
Oxygen
Carbon monoxide
Sulfur dioxide
Formaldehyde
Analytes

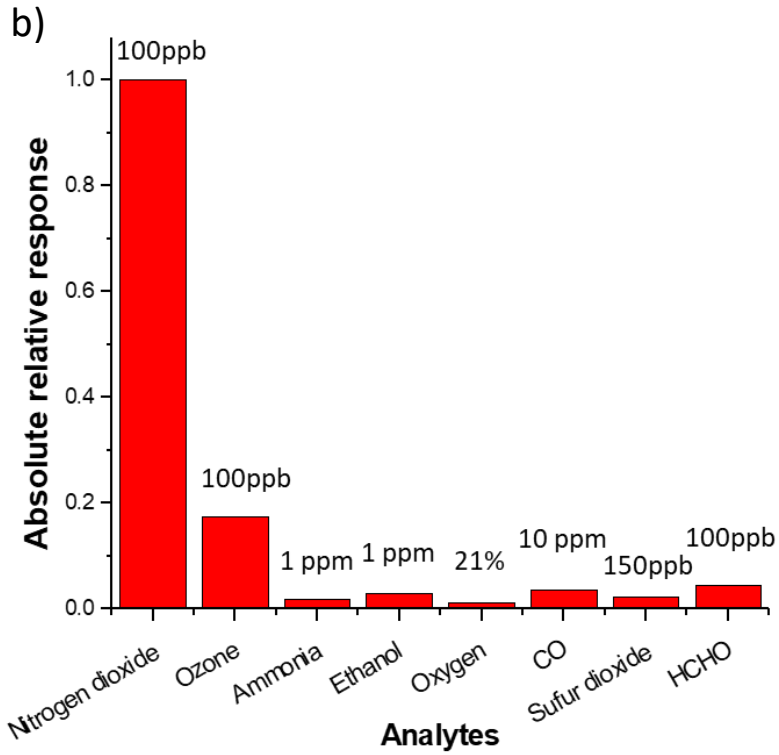
b)
100ppb
Absolute relative response
1.0
0.8
0.6
0.4
0.2
0.0
100ppb
1 ppm
1 ppm
21%
10 ppm
150ppb
100ppb
Nitrogen dioxide
Ozone
Ammonia
Ethanol
Oxygen
CO
Sufur dioxide
HCHO
Analytes

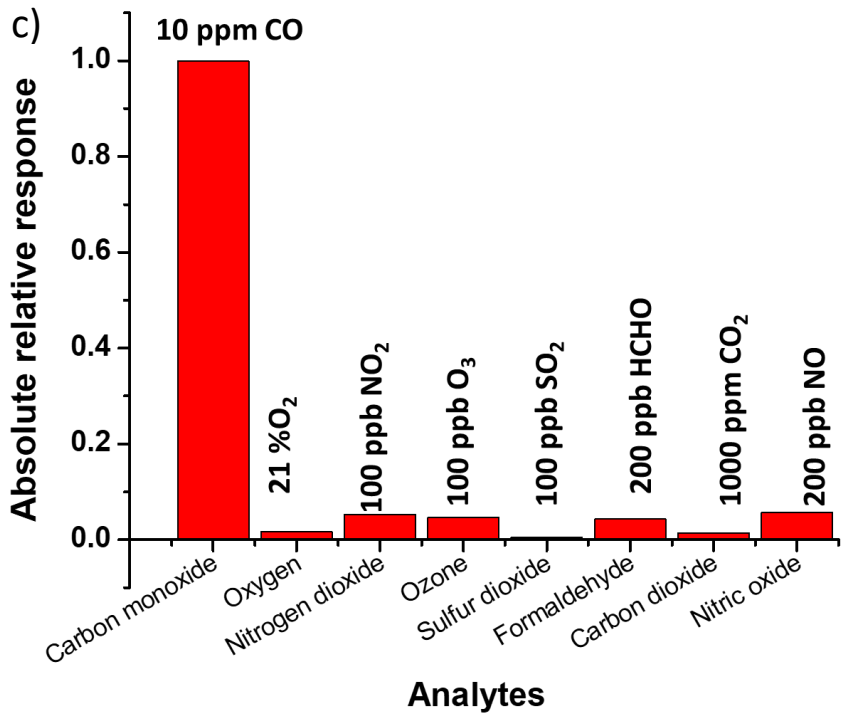

Figure 3.6 Cross-sensitivity test of (a) O_3 sensor (b) NO_2 (c) CO sensor with other common interferents.

3.4.4 Sensor lifetime

Conventional colorimetric sensors are usually one-time use only since most of the sensing probes will be consumed during the detection, like the colorimetric gas detector tubes, pH test papers, and humidity indicators. This is because 1) there is no control of the mass transportation of the exposure of analyte to the sensing probes, usually based on passive diffusion; and 2) the qualitative or quantitative detection of the analyte is based on visual checking with human eyes, thus reliable detection depends on tremendous amount of chemical reaction between analytes and sensing probes. In order to save the sensing

probes while improving the detection limit and sensitivity, A miniaturized pump was applied to actively deliver the sample gas at a constant flow rate within a short period of time and a CMOS imager was used to sensitively and reliably monitor the color development during the detection. This design has made it possible to use the same sensor for multiple and continuous measurements. Again, here we use CO sensor as an example, as shown in Fig.3.7, multiple consecutive injections have been performed on the same CO sensor chip by alternating the purging and sensing period. The reproducibility of the consecutive measurement is evaluated by calculating the variability of 5 sensor responses to 10 ppm CO at 75%RH, and the variation is less than 6%, indicating excellent sensing reliability and capacity. The consecutive sensing plots also indicate that the sensing mechanism is not reversible. When the injection stops, the optical intensity also stops changing until a new injection happens. The irreversibility comes from the high selectivity of the reaction and high stability of the product, both of which are essential for the high performance of the colorimetric CO sensor. Results indicated in Fig.3.7 also imply that the continuous CO monitoring can be achieved even with a single sensor chip. We have tested the sensing capacity of the sensor chip we prepared, and it can reach 8 ppm·hour, a dose the sensor can take before its sensitivity drop by 10%. Assuming the CO concentration in the ambient air is 10ppm, (WHO standard, 10 ppm (8-hour mean)), and the sampling time is 20s, the CO sensor chip can be used for 150 times before replacement.

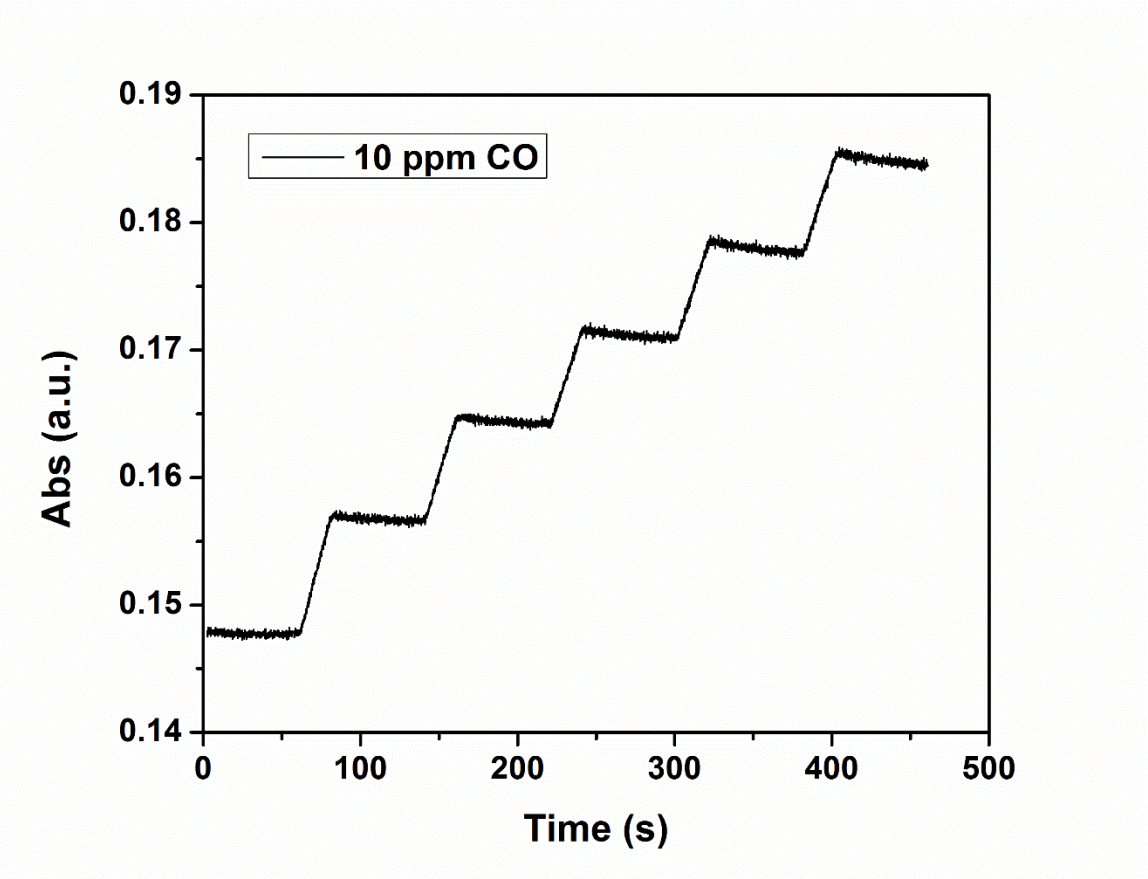

Figure 3.7 The CO sensor response during continuous monitoring of 10 ppm CO at 75% RH (60 seconds purging and 20 seconds sampling). The variation of sensor response among different sampling periods was less than 6%.

3.5 Conclusion

By introducing the optical detection system (including a light source and a CMOS imager), active sample delivery system, and flat sensor chip geometry, a high-performance gas sensing platform has been successfully designed and constructed. The fast, specific, and irreversible colorimetric reaction between target analytes and sensing probes provides the chemical sensor with fast response, high selectivity, and high reliability. The high

loading capacity of sensing probes on the porous substrate, the sensitive optical detector, and the optimized sampling rate make the sensor suitable for personal exposure monitoring.

References

[65] Dominici, F.; Peng, R. D.; Barr, C. D.; Bell, M. L., Protecting human health from air pollution: shifting from a single-pollutant to a multipollutant approach. *Epidemiology (Cambridge, Mass.)* **2010,** *21* (2), 187-194.

[66] Dons, E.; Laeremans, M.; Orjuela, J. P.; Avila-Palencia, I.; Carrasco-Turigas, G.; Cole-Hunter, T.; Anaya-Boig, E.; Standaert, A.; De Boever, P.; Nawrot, T.; Götschi, T.; de Nazelle, A.; Nieuwenhuijsen, M.; Int Panis, L., Wearable Sensors for Personal Monitoring and Estimation of Inhaled Traffic-Related Air Pollution: Evaluation of Methods. *Environmental Science & Technology* **2017,** *51* (3), 1859-1867.

[67] Hu, K.; Davison, T.; Rahman, A.; Sivaraman, V., Air Pollution Exposure Estimation and Finding Association with Human Activity using Wearable Sensor Network. In *Proceedings of the MLSDA 2014 2nd Workshop on Machine Learning for Sensory Data Analysis*, ACM: Gold Coast, Australia QLD, Australia, 2014; pp 48-55.

[68] Tsow, F.; Forzani, E.; Rai, A.; Wang, R.; Tsui, R.; Mastroianni, S.; Knobbe, C.; Gandolfi, A. J.; Tao, N. J., A Wearable and Wireless Sensor System for Real-Time Monitoring of Toxic Environmental Volatile Organic Compounds. *IEEE Sensors Journal* **2009,** *9* (12), 1734-1740.

[69] Rai, P.; Kim, Y.-S.; Song, H.-M.; Song, M.-K.; Yu, Y.-T., The role of gold catalyst on the sensing behavior of ZnO nanorods for CO and NO_2 gases. *Sens. Actuators, B* **2012,** *165* (1), 133-142.

[70] Yanagimoto, T.; Yu, Y. T.; Kaneko, K., Microstructure and CO gas sensing property of Au/SnO_2 core–shell structure nanoparticles synthesized by precipitation method and microwave-assisted hydrothermal synthesis method. *Sens. Actuators, B* **2012,** *166–167*, 31-35.

4 GRADIENT-BASED COLORIMETRIC SENSORS WITH GREATLY EXTENDED LIFETIME

4.1 Introduction

Monitoring of air quality, studying of environmental health, and protection of people from harmful chemical exposures have motivated increasing efforts to develop low cost and high performance chemical sensors. These efforts include development of miniaturized metal oxide semiconductor and electrochemical sensors, which represent current mainstream commercial gas sensors. [71-77] Colorimetry is another well-known sensing principle that is also widely used in commercial gas sensors. It detects a color change associated with a specific chemical reaction between an analyte and sensing materials. A distinct feature of colorimetric sensing is its capability for parallel sensing of multiple analytes when used in an array format. Because most colorimetric reactions are irreversible, today's commercial colorimetric sensors are typically for one-time use, and for qualitative or semi-quantitative analysis only.[13] For these reasons, colorimetric sensors are not suitable for applications that require continuous and reliable quantitative sensing.

To overcome the drawbacks of colorimetric sensing, in the previous chapter, we reported colorimetric gas detection by actively controlling the exposure dose of sensing elements to gas analyte during each detecting cycle.[78] When the exposure time is limited to 20 s, the sensor chip can be used for 150 times before replacement. Despite the success, these methods still fall short for continuously tracking of analytes. Here we introduce a gradient-based colorimetric sensor (GCS) to achieve sensitive, quantitative, and

continuous gas monitoring. We present the principle of GCS, build a prototype device, carry out experiments, validate the experimental results with numerical simulations, and demonstrate continuous detection of ozone in real-time.

4.2 Detection principle and setup

The key component of GCS is a sensor chip consisting of a sensing probe-coated porous substrate covered with a top layer to prevent exposure of the sensing probe to analyte from the top (Fig. 4.1(a)). When the analyte diffuses along the porous substrate from one edge, it starts to react with the sensing probe at the location of its first contact and changes the local color of the porous substrate, which creates a color gradient along the substrate (Fig. 4.1(a)). The gradient shifts laterally over time when the sensor chip is exposed to the analyte continuously. GCS measures the position of the maximum gradient, and tracks its lateral shift over time with sub-micron precision, leading to sensitive and continuous monitoring of the analyte.

To demonstrate GCS, we used indigo carmine as the sensing probe, which reacts specifically with O_3. O_3 is one of the six EPA listed "criteria" air pollutants,[6] and is harmful to human lung function and respiratory system, causing various diseases, such as asthma, bronchitis, and heart attack.[79-80] The porous material was made of silica gel to provide a large surface area for sensitive colorimetry and allow O_3 to diffuse along the porous substrate from one end (inlet) to another (outlet). The top layer was an acrylic sealing plate, which helped confine O_3 diffusion along the porous substrate. O_3 reacted with sensing probes near the inlet initially, and then with the probes along the GCS over

time as the sensing probes near the inlet depleted upon irreversible chemical reaction. The unreacted sensing probe for O_3 detection was blue (Fig. 4.1(a)), which turned into white after complete reaction with O_3. The region that separated the reacted (white) and unreacted (blue) sensing probes was described by a color gradient (Fig. 4.1(b)). The color gradient shifted from left to right upon continuous exposure to O_3, and the rate that the gradient position shifted over time reflected O_3 concentration. GCS tracked the shift in the gradient position Δx) by analyzing the intensity profile captured with a CMOS imager. We will show later that the gradient shift (Δx) at time t is directly related to O_3 concentration.

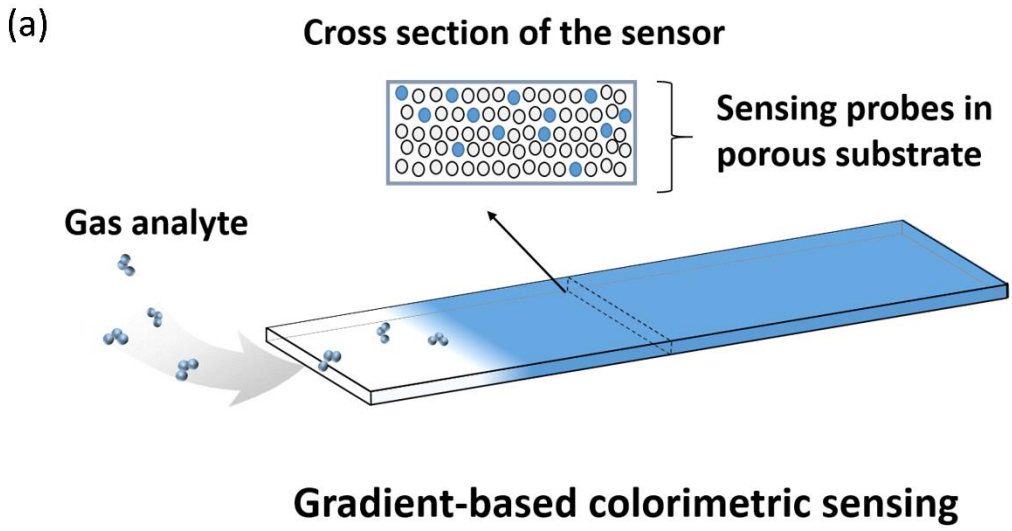

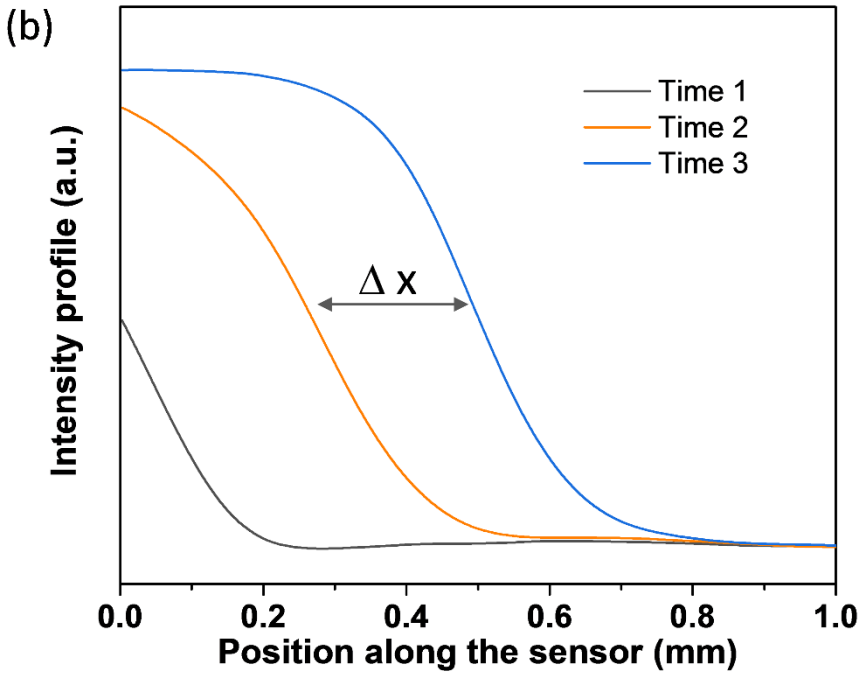

Figure 4.1 (a) Schematics of GCS. A porous substrate is coated with a sensing probe that can react with an analyte specifically and change color. The top of the porous substrate is covered with a layer of acryl to prevent direct exposure of the sensing probe to the analyte from the stop, such that the analyte can only diffuse from the edge of the substrate to react with the sensing probe. The local reaction creates a color gradient, and GCS tracks the color gradient shift along the substrate over time. (b) Snapshots of the intensity profiles showing shifting of the color gradient over time.

4.3 Experimental

4.3.1 Reagents and sensor preparation

Indigo carmine and citric acid were purchased from Sigma-Aldrich, Inc., which were dissolved in ultra-pure water (18 MΩ) containing glycerol. The solutions were cast onto silica gel substrates, purchased from Sorbent Technologies (Polyester backed silica G TLC plates). O_3 samples with concentrations from 10 to 500 ppbV were generated by an O_3 generator (UVP Corp.) using UV radiation. The actual concentration of each O_3 sample was confirmed by an O_3 analyzer (2B Technologies, Inc.).

4.3.2 Chemical reactions

The present micro-colorimetric O_3 sensor is based on the chemical reaction of O_3 with indigo carmine, which is blue at pH<11.4. The reaction product is colorless isatin sulfonic acid.

4.3.3 Optimization of sensor configuration

A GCS chip with dimensions of 4 mm (length) x 0.5 mm (width) x 250 μm (thickness) was cut from silica gel substrates by a laser cutter (Universal Laser Systems). The sensor was coated with a layer of sensing probes (indigo carmine for O_3) and then covered with a flat piece of Acrylic to prevent exposure of the sensing probes from the top. The GCS chip was illuminated with a white LED (LEDtronics Inc.) and imaged with a CMOS imager (Logitech, Inc.) for real-time monitoring of the color gradient continuously when exposed to the gas analyte (Fig. 4.1(a)).

4.3.4 Optical gradient-tracking method

A key task in GCS is to detect and track the gradient shift. We achieved this task by developing a sensitive imaging-processing algorithm from the time sequence images captured with a CMOS imager. The algorithm determines the position of the maximum color gradient with the following steps (Fig. 4.2): 1) Extract the intensity profile from the captured images; 2) Find the maximum (Max) and minimum (Min) intensity values from the intensity profile; 3) Determine the position on the intensity profile where the intensity equals the mean value, Mid= (Max+ Min)/2; 4) Track the position over time. Note that the image in the background of Fig. 4.2was used to show the actual color gradient corresponding to the intensity profile. To validate this method for continuous tracking of O_3 concentration, we calibrated the O_3-GCS sensor based on the speed of gradient shift at various concentrations of O_3. The results in Fig. 4.3 show a linear dependence of the gradient shift speed on O_3 concentration over a large concentration range, from 0 to 500 ppb. This concentration range covers most of the personal O_3 exposure monitoring applications. From the slope of the calibration, we determined the sensitivity of the O_3 sensor to be $(1.14\pm 0.06) \times 10^{-7}$ mm/s/ppb (R^2= 0.99).

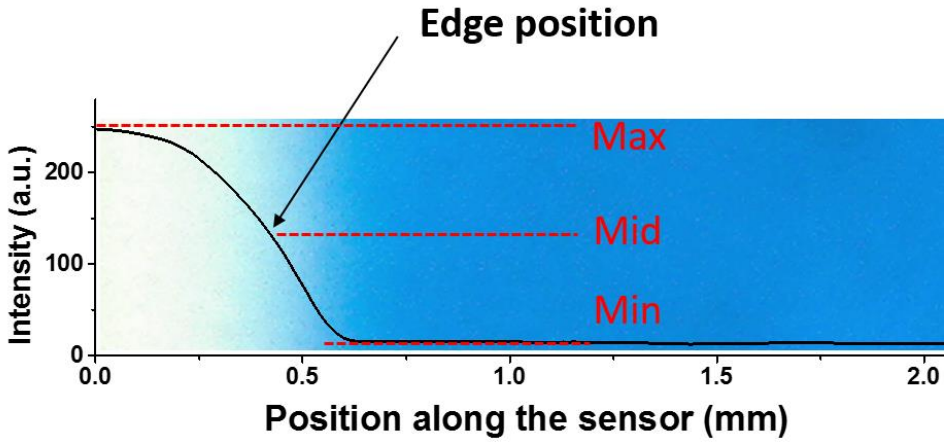

Figure 4.2 Image of the partially reacted sensor and corresponding intensity profile of the sensor. The optical tracking method finds the maximum (Max) and minimum (Min) value to calculate the mid-value and searches the position along the sensor that has the intensity value closest to Mid, and finally defines the position as the "gradient position".

4.4 Simulation

To validate the GCS principle and guide the design of a GCS sensor, we simulated O_3 mass transport and chemical reaction kinetics along the porous substrate numerically. The O_3 probe is indigo carmine, which is blue at pH<11.4. The reaction product is isatin sulfonic acid, a colorless substance. We confirmed this reaction by measuring the UV-visible spectra of indigo carmine before and after exposure to O_3, and found that the reaction of indigo carmine with O_3 led to a decrease of optical absorbance at ~600 nm.

We denote the reaction as, c (g) + n (s) → p (s), where c is the O_3 concentration in the air sample, n is the density of reaction sites or sensing probes (indigo carmine) available for the reaction on the O_3 sensor, and p is the concentration of the reaction product. The diffusion and reaction kinetics are described by

$$\frac{\partial c}{\partial t} + \nabla \cdot (-D\nabla c) = R \quad (1)$$

$$R = \frac{\partial n}{\partial t} = -kcn\,, \quad (2)$$

where k is the reaction rate coefficient, R is the reaction rate, and D is the diffusion coefficient of O_3 in the porous silica gel substrate (D= 1.1×10^{-11} m^2/s). We assumed the following boundary conditions: c(inlet, t)=c_0, where c_0 is the concentration of the air sample; c(outlet, t)=0, implying a sufficient long GCS sensing chip; the concentration (c) is continuous at the interface of air-silica substrate, and $\frac{\partial c}{\partial n}$, the concentration gradient, on the top and side walls are zero (reflecting zero flux of O_3 or perfect sealing).

Solving Eqs. (1) and (2) with the boundary conditions defined above allows us to determine c and n along the channel. The color change is proportional to p (product), which is related to n by p=n_0-n, where n_0 is the initial concentration of the O_3 sensing probes. In other words, the depletion of the O_3 sensing probes equals the generation of the reaction product. The simulation shows that the color changes when exposing the sensor to 500 ppbV O_3 for different time durations (Fig. 4.3(a)). Note that the blue bars represent the cross-section of a GCS along the direction from the inlet to outlet and the white color represents the consumption of the sensing probes at a specific location along the sensor. The concentration profiles along the sensor provide local optical intensity (color change) along the channel (Fig. 4.3(b)). We note that the simulation results shown in Fig. 4.3 were

obtained by taking k=100 $m^3/(s \cdot mol)$. This value was chosen by comparison of simulation and experimental results obtained with a sensing surface without mass transport limitations.

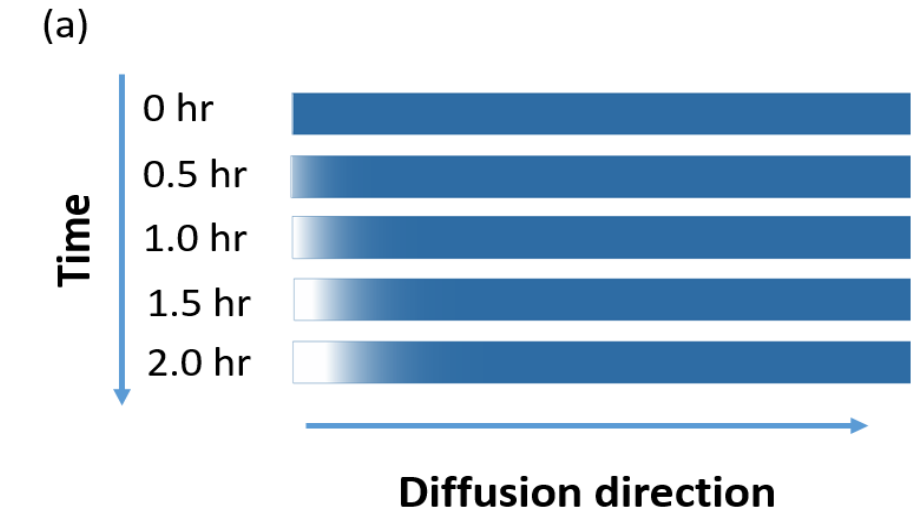

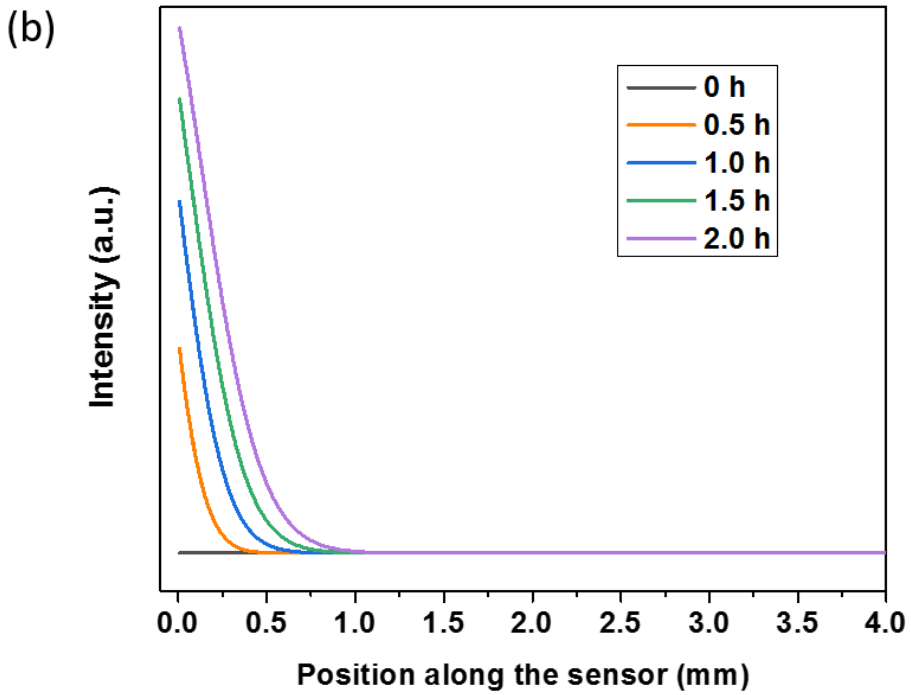

Figure 4.3 Simulated gradient shifts upon continuous exposure to O_3 over 2 hours. (a) Simulated concentration profiles of unreacted O_3 sensing probe (indigo carmine, blue color) when exposed to 500 ppbV O_3 for 0, 0.5, 1, 1.5, and 2 hours, respectively. (b) Simulated intensity profile (color gradient) along the sensor (colored solid lines).

4.5 Results and Discussion

4.5.1 Validation of the simulation

To experimentally validate GCS for continuous monitoring of O_3, we tested the sensor by exposing the sensor to 500 ppbV O_3 over 2 hours and observed gradual color development along the sensor (Fig. 4.3). The measured color changes at different locations over time as shown in Fig. 4.3 are consistent with the simulated results in Fig. 4.3 (a), indicating the diffusion-reaction equations and the boundary conditions provide a reasonable description of the O_3 sensor. The simulation and experiment also show that GCS with passive sampling (diffusion) can continuously track O_3 in the air. The lifetime of the sensor can be determined from the gas analyte concentration and the sensor's sensing capacity -- the maximum amount of analyte a sensor can detect over a given time interval. In the present O_3 sensor, the capacity was determined to be 7 ppmV·hour, indicating that it can continuously monitor 100 ppbV O_3 for 70 hours. The EPA O_3 exposure limit is 70 ppbV over 8 hours averaging time, and O_3 concentration in typical ambient air is usually much lower than the EPA standard.

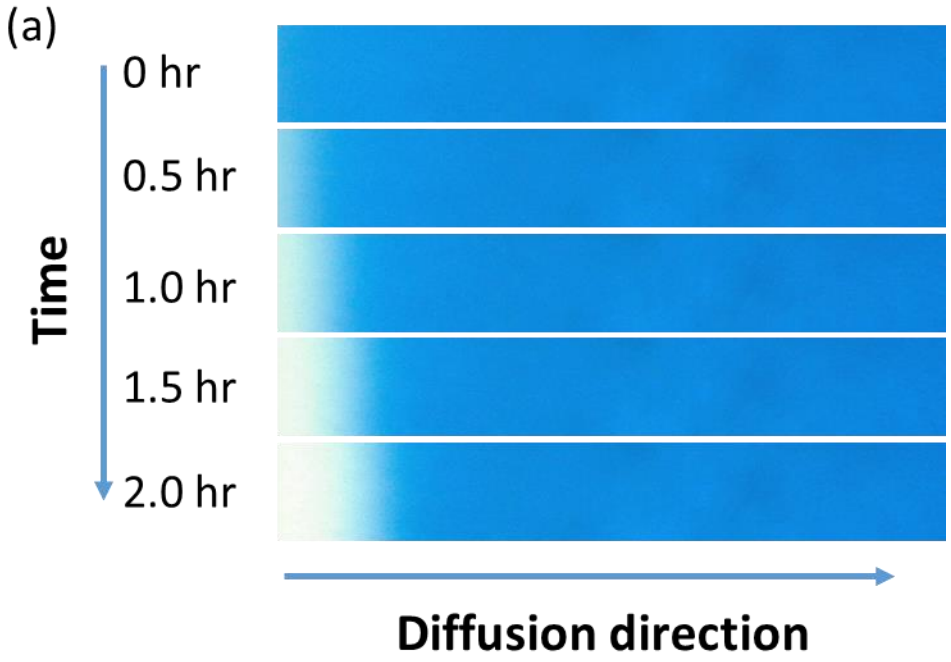
(a)
0 hr
0.5 hr
1.0 hr
1.5 hr
2.0 hr
Time
Diffusion direction

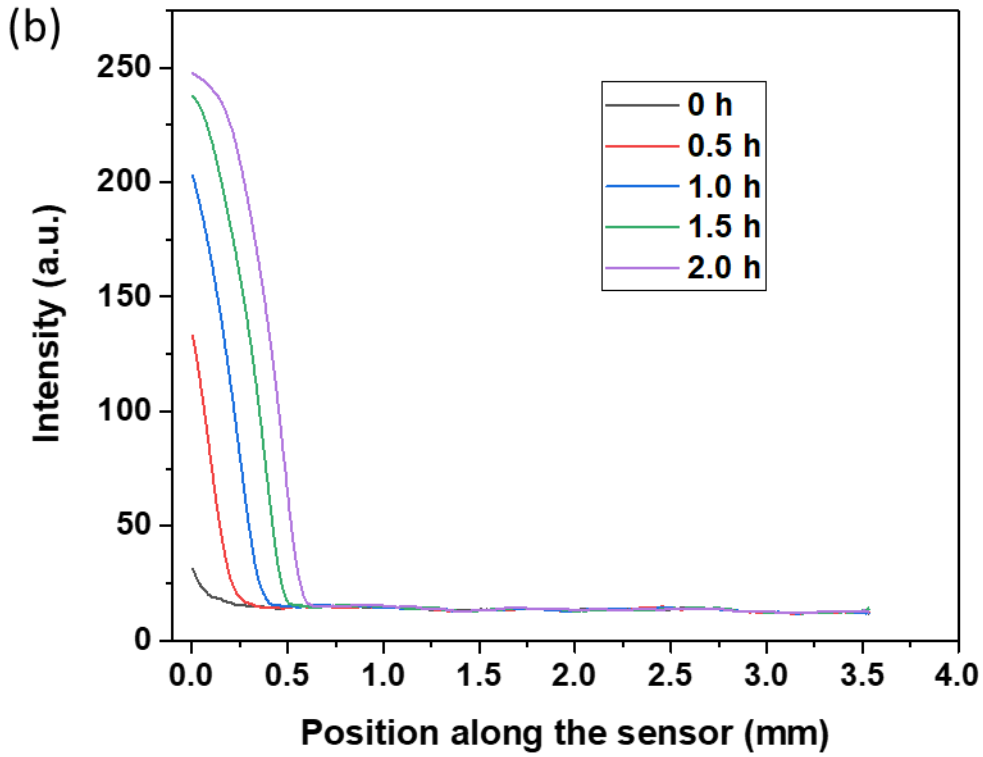
(b)
Intensity (a.u.)
Position along the sensor (mm)
0 h
0.5 h
1.0 h
1.5 h
2.0 h
0
50
100
150
200
250
0.0
0.5
1.0
1.5
2.0
2.5
3.0
3.5
4.0

Figure 4.4 Measured gradient shifts upon continuous exposure to O_3 over 2 hours. (a) Measured images with the CMOS imager showing color gradient development over 2 hours at 500 ppb O_3. (b) Measured intensity profile (color gradient) shifts along the sensor surface over time.

4.5.2 Sensitivity and dynamic range

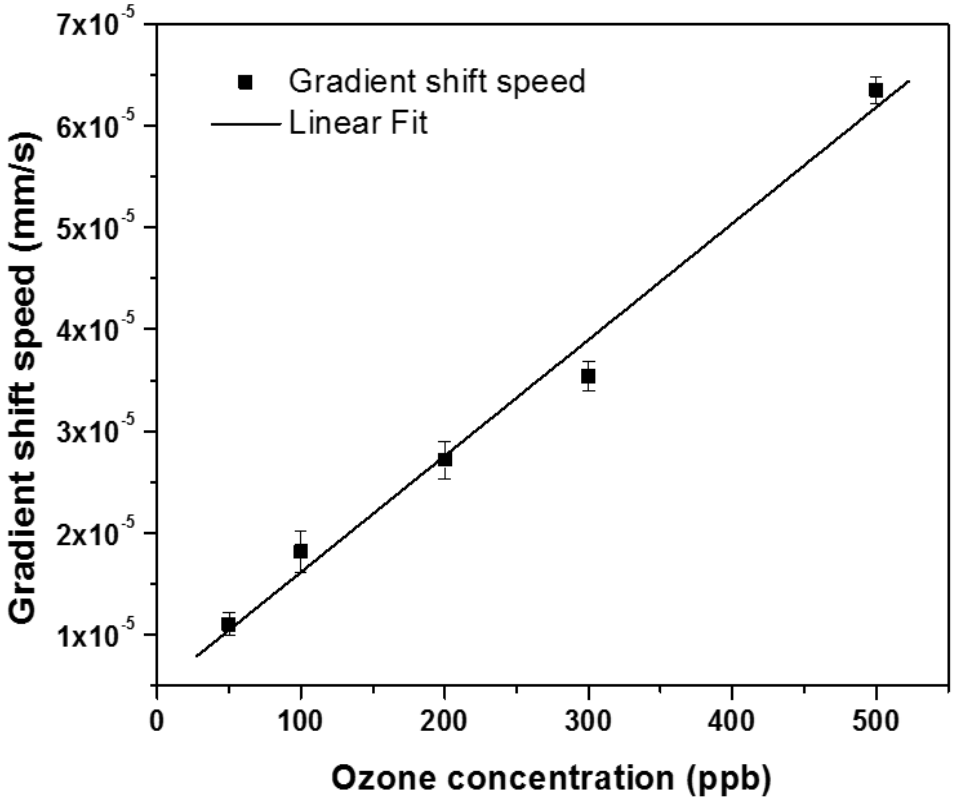

Figure 4.5 Calibration of the O_3-GCS with a reference O_3 analyzer, showing a linear dependence of the sensor response (gradient shift speed) to O_3 concentration.

4.5.3 Sensor response time

When choosing gas sensors for a given application, detection limit (DL), response time (τ), and lifetime are important parameters. Because GCS measures the lateral shift (Δx) in the color gradient, the detection limit of GCS is determined by how precisely we can track the position of the color gradient. If we define this precision as 3 times of the noise level (σ^2) of the position tracking, and then DL is given

$$DL = \frac{3\sigma^2}{\tau S} \qquad (3)$$

where S is the sensitivity of GCS determined by the slope of Fig. 4.4. Eq. 3 shows that DL is inversely proportional to τ, so one may improve detection limit by increasing measurement time (allowing sufficient accumulation of gradient shift). However, for a given measurement time, we must minimize the noise level in the tracking of gradient shift. We discuss below the dependence of the noise level on different factors.

The noise level in the gradient position (δx) is related to the color gradient ($\frac{dI}{dx}$) and noise level of the intensity (color)(δI), given by

$$\delta x = (\frac{dI}{dx})^{-1}\delta I. \qquad (4)$$

If the gradient is sharp, dI/dx is large, so is δx, which favors a lower detection limit. On the other hand, if the gradient is smooth, the detection limit will be poor. The sharpness of the gradient is related to the substrate porosity. So the selection of a suitable substrate is of great importance. In the present work, we chose a silica substrate with pore diameter, 6 nm, and pore volume, ~ 0.75 ml/g. The position-tracking position defined by 3x standard deviation is ~0.08 μm. The corresponding detection limit is 10 ppb for a response time of 3.5 min.

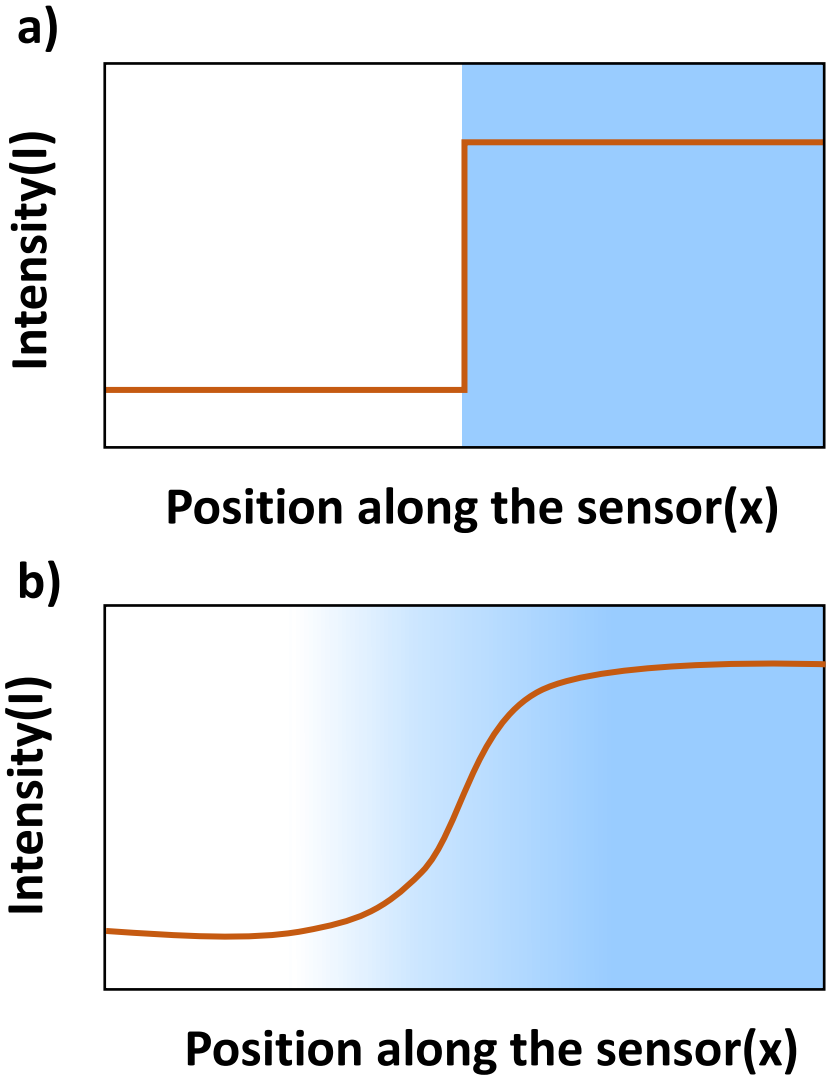

Figure 4.6 (a) Illustration of a sharp and (b) smooth gradient along a GCS.

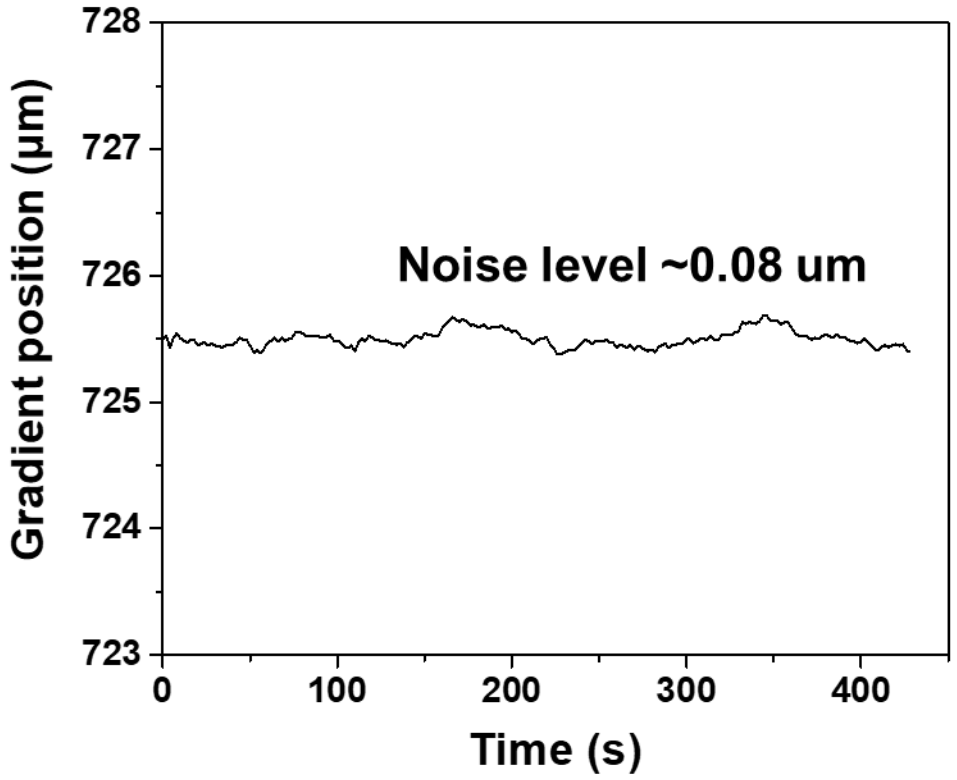

Figure 4.7 Gradient position tracking noise level of an O_3-GCS when testing clean air. The noise level is ~0.08 μm.

4.5.4 Sensor lifetime

For continuous monitoring of air quality, one wishes to achieve long lifetime, which is determined how fast the sensing probes are consumed (reacted with the analyte) along the entire GCS surface. This is related to the sensor length, the density of the sensing probes and concentration of the analyte. For our O_3-GCS, as mentioned in section 2, the length is 4 mm, which can continuously monitor 100 ppbV O_3 for 70 hours. Longer sensor lifetime

should be possible by increasing the length of the sensor, and the density of the sensing probes.

4.6 Conclusion

We have developed GCS to overcome the difficulty of traditional colorimetric sensors that are limited to one-time use only due to irreversible color-change producing chemical reactions. We have fabricated an O_3-GCS device and shown reliable detection of O_3 via passive sampling (without using air pumps). Removing the use of air pumps is critical for miniaturization of the size and power consumption of the device. We have carried out a numerical simulation of the GCS with passive air sampling and found that it is in good agreement with the experimental data, indicating the gas sensing process can be described with diffusion and reaction processes. We have also developed an optical gradient-tracking technique to detect the gradient shift over sub-micron precision, which allows the O_3-GCS to reach a detection limit of 10 ppbV (with 3.5 min sampling). The sensor lifetime is 7 ppmV·hour, corresponding to continuous detection of 100 ppbV O_3 for 70 hours without sensor replacement.

References

[6] National Ambient Air Quality Standards. https://www.epa.gov/criteria-air-pollutants/naaqs-table#3.

[13] *Dräger-Tube/CMS Handbook: Handbook for short term measurements in soil, water and air investigations as well as technical gas analysis.* 16th Edition ed.; Dräger Safety AG & Co KGaA: Lübeck, 2011; p 225.

[71] Lewis, A.; Edwards, P., Validate personal air-pollution sensors. *Nature* **2016,** *535* (7610), 29-31.

[72] Wetchakun, K.; Samerjai, T.; Tamaekong, N.; Liewhiran, C.; Siriwong, C.; Kruefu, V.; Wisitsoraat, A.; Tuantranont, A.; Phanichphant, S., Semiconducting metal oxides as sensors for environmentally hazardous gases. *Sensors and Actuators B: Chemical* **2011,** *160* (1), 580-591.

[73] Li, J.; Lu, Y.; Ye, Q.; Cinke, M.; Han, J.; Meyyappan, M., Carbon Nanotube Sensors for Gas and Organic Vapor Detection. *Nano Letters* **2003,** *3* (7), 929-933.

[74] Vallejos, S.; Khatko, V.; Aguir, K.; Ngo, K. A.; Calderer, J.; Gràcia, I.; Cané, C.; Llobet, E.; Correig, X., Ozone monitoring by micro-machined sensors with WO_3 sensing films. *Sensors and Actuators B: Chemical* **2007,** *126* (2), 573-578.

[75] Kamionka, M.; Breuil, P.; Pijolat, C., Calibration of a multivariate gas sensing device for atmospheric pollution measurement. *Sensors and Actuators B: Chemical* **2006,** *118* (1), 323-327.

[76] Koutrakis, P.; Wolfson, J. M.; Bunyaviroch, A.; Froehlich, S. E.; Hirano, K.; Mulik, J. D., Measurement of ambient ozone using a nitrite-coated filter. *Analytical Chemistry* **1993,** *65* (3), 209-214.

[77] Peterson, P.; Aujla, A.; Grant, K.; Brundle, A.; Thompson, M.; Vande Hey, J.; Leigh, R., Practical Use of Metal Oxide Semiconductor Gas Sensors for Measuring Nitrogen Dioxide and Ozone in Urban Environments. *Sensors* **2017,** *17* (7), 1653.

[78] Lin, C.; Xian, X.; Qin, X.; Wang, D.; Tsow, F.; Forzani, E.; Tao, N., High Performance Colorimetric Carbon Monoxide Sensor for Continuous Personal Exposure Monitoring. *ACS Sensors* **2018,** *3* (2), 327-333.

[79] Lewis, A. C.; Lee, J. D.; Edwards, P. M.; Shaw, M. D.; Evans, M. J.; Moller, S. J.; Smith, K. R.; Buckley, J. W.; Ellis, M.; Gillot, S. R.; White, A., Evaluating the performance of low cost chemical sensors for air pollution research. *Faraday Discussions* **2016,** *189* (0), 85-103.

[80] Bernstein, M.; Whitman, D., The Challenges of Battling Ozone Pollution. *Environment: Science and Policy for Sustainable Development* **2005,** *47* (8), 28-41.

5 A MINIATURIZED, INTEGRATED GRADIENT-BASED COLORIMETRIC ARRAY FOR ENVIRONMENTAL MONITORING

5.1 Introduction

As mentioned in the earlier chapter, with urbanization and industrialization occur at an unprecedented rate, air pollution has become a serious problem for human society. It has been reported that air pollution is linked to various health issues, for example, short term exposure to air pollution causes nausea, headaches, and irritation of the upper respiratory tract, whereas long term exposure leads to respiratory diseases, lung cancer and heart diseases. This makes it necessary and urgent to accurately monitor air pollution level including indoor and outdoor air pollution to help people aware of air pollution exposure and further help prevent any air pollution-related health risks.

Asthma is one of the most common respiratory diseases in the United States, with 14% of children diagnosed with asthma. [26] Asthma has a range of symptoms that can sometimes be debilitating. Symptoms include shortness of breath, coughing, feeling tired, allergies and chest pain.[81] Since asthma patients are extremely sensitive to environmental contaminants, exposure to these contaminants triggers an asthma attack, so it is important for epidemiologists to understand the micro-environment around patients. Therefore, sensors capable of continuously monitoring the real-time concentration levels of key asthma triggers, such as O_3, NO_2 and formaldehyde, are extremely useful for the control and prevention of asthma.

Existing analytical chemistry equipment that can separate and analyze these target chemicals, such as GC-MS, which can separate analyte samples, identify chemicals, and

quantify the concentration of each chemical. The method is accurate, but the main disadvantages are large size, expensive and inability to perform on-site analysis, which cannot be used as a method for personal exposure monitoring.

There are also small and relatively inexpensive techniques to monitor these triggers, such as MOS sensors and electrochemical sensors.[82-86] For MOS sensors, due to their material properties, the sensors required to be heated up to a certain high temperature, which has relatively high power consumption. In addition, the signal of the MOS sensor drifts with time, so it is necessary to recalibrate after long-term use. Therefore, to use MOS sensors, a series of compensation and recalibration is required, which is not desirable for the target application. Electrochemical sensors are selective and accurate, but they are generally expensive, and face the problem of signal drift over time like MOS sensors because of the electrolyte depletion.[87] Recalibration and signal drift over time are extremely undesirable since the sensor is supposed to be used by people in general and no extra recalibration should be required.

Colorimetric sensors are popular due to their unique advantages such as good selectivity, cost-effective, calibration-free. All of these characteristics make colorimetric sensors ideal for targeted applications. However, colorimetric sensors face a critical disadvantage of short sensor life. The sensor usually can only be used for one time.[13] Once exposed, colorimetric sensors are typically consumed within hours, making it difficult to continuously monitor asthma triggers.

The colorimetric sensors described in the previous chapters overcome the drawback of traditional colorimetric sensors and showed great capability of continuous personal

exposure monitoring. However, to be used in real application, the sensor fabrication and assembly should be as simple as possible for mass production. Current gradient-based colorimetric sensors required to be covered with a flat piece of Acrylic to prevent exposure of the sensing probes from the top and sensors for different target analytes need to be assembled respectively, which takes up a lot of space when being installed in a device. A sensor that integrated multiple sensing elements and can be easily assembled is highly preferred.

Inkjet printing technology is not only an office printing technology but has gradually become a useful tool for various industrial fabrication processes. It can accurately deposit very small droplets of materials at defined spots on various substrates. Currently, this technology has been widely used in the manufacture of plastic electronic products and polymer light-emitting diodes (LEDs).[88-90] Inkjet printing is also becoming a timesaving, cheap alternative to photolithography because it allows for the formation of patterns directly on the surface of the substrate compared to the process of lithography. It does not rely on the use of specific masks, and clean room facilities are not a prerequisite. In addition, inkjet printing has become another arranging technique for biological sample arrays, which has the advantage of reducing contamination and no risk of substrate damage compared to contact-based methods.

In this chapter, an inkjet printing method using a cheap home printer has been developed to integrate several gradient-based colorimetric sensors together on one sensor substrate. An easily assembled sensor cartridge has also been designed to make sensor replacement as simple as possible. The printed gradient-based colorimetric sensor has been

calibrated and the printed ozone sensor has been tested in real tests, proving the ability of the sensor to be used for continuous personal exposure monitoring.

5.2 Experimental

5.2.1 Reagents and setup

Sulfanilamide (SFA), N, N-dimethyl-1-naphthylamine (DMNA), glycerol, hydroxylamine sulfate, thymol blue, methanol, indigo carmine, citric acid, 1-propanol were purchased from Sigma-Aldrich, lnc. Ultra-pure water (18MΩ) was produced by an ELGA Purelab Ultra RO system. Silica gel substrates were purchased from Sorbent Technologies (Silica G TLC Plates, Polyester Backed, 20×20 cm, 250 μm thickness, 60 Å mean pore diameter of silica gel, pore volume: ~ 0.75 ml/g, specific surface area: ~ 500 m^2/g). The substrate was cut into 5×5 mm pieces by laser cutter and wash with DI water and ethanol for three times, respectively. An Epson XP-340 printer was used to print the sensing nmaterials on the sensor substrate.

5.2.2 Inkjet printing for sensor preparation

NO_2 sensor printing solution: the printing solution was prepared by dissolving 400 mg of 200 uL of DMNA in the 40 mL mixture of 1-propanol and water (volume ration of 1.5:1) solution with 2 ml glycerol.

O_3 sensor printing solution: the printing solution was prepared by dissolving 36 mg indigo carmine and 2.8 g citric acid in a solvent mixture containing 20 mL of DI and 20 mL 1-propanol with 2 ml glycerol.

HCHO sensor: the printing solution was prepared by dissolving 400 mg hydroxylamine sulfate and 24 mg thymol blue in a solvent mixture containing 1-propanol, water, and glycerol (volume ration of 12:8:1). 400 uL NaOH solution (1M) was added to adjust solution pH.

The solutions were injected into the empty printer cartridge and then inkjet-printed onto the substrate. The Epson XP-340 home printer was controlled by a laptop and a printing pattern was created using CorelDRAW software. The printing process was repeated 10 times to achieve a better sensitivity of the sensor chip.

All sensors were vacuum-dried completely after printing to remove any 1-propanol residue. The sensors were kept under dry nitrogen atmosphere for 20 min to keep get rid of moisture on the silica gel substrate before sealing into the black pouch. Store sensors in the refrigerator.

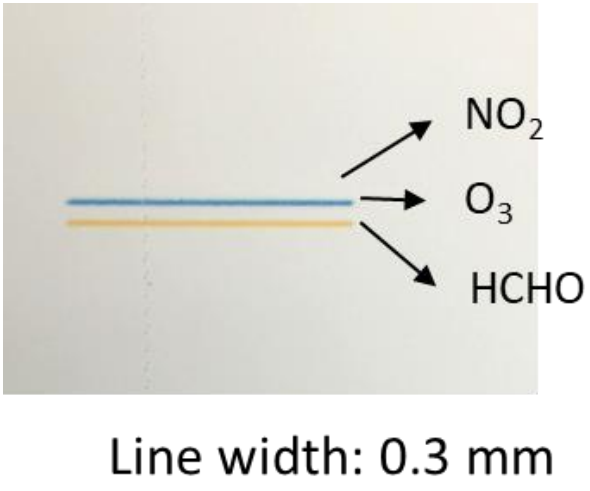

Figure 5.1 Three printed sensors (NO_2, O_3 and HCHO sensors) with a line width of only 0.3 mm on a silica gel substrate.

5.2.3 Sensor assembling methods

Figure 5.2 shows different sensor assembly methods that have been compared in this work. The sensor assembled directly by tapes suffered from sensor degradation because different tapes released different chemicals that cause a color change as shown in Figure 5.2 (a). The color of a printed HCHO sensor turns pink when using scotch tape and it turns more yellow when using transparent duct tape. Figure 5.2 (b) shows a screw mechanical assembly method which is too bulky, and it required a screwdriver to assemble it. Fig 5.2(c) shows the newly design one-piece assembling 3D printed holder and a schematic of how the sensor clipper work to guarantee 1D diffusion from the side view.

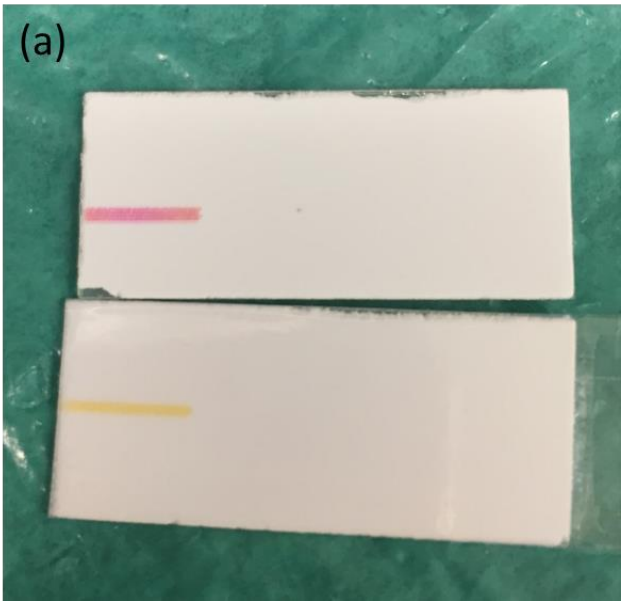
(a)

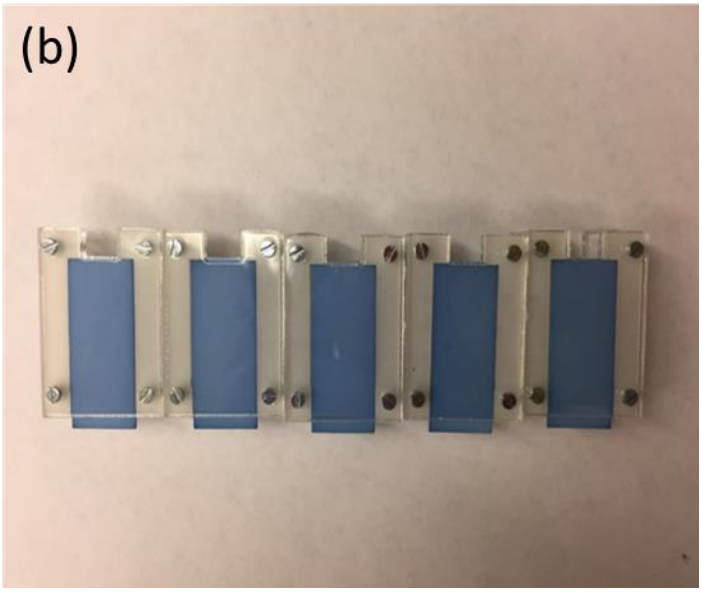
(b)

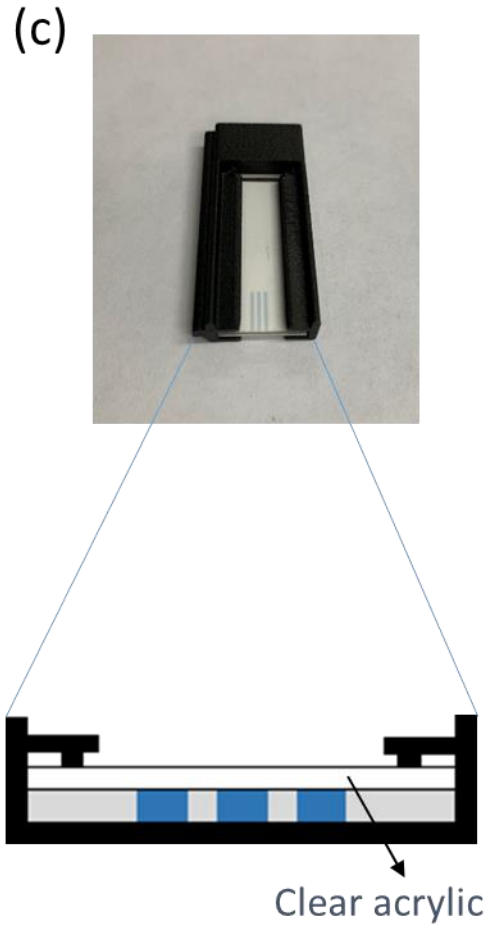

Figure 5.2 Different sensor assembly methods.

5.2.4 Image processing methods

The image processing method is the same with edge-tracking method being used for the gradient-based colorimetric sensors in the previous chapter. The location of the maximum color gradient along a sensor was defined as an “edge”. The method was designed for the colorimetric sensing to determine the edge position by the following steps:

1) Extract intensity profile from the captured image by CMOS imager; 2) Find the maximum and the minimum intensity value along the sensor and calculate Mid= (Max+ Min)/2; 3) Track the positions along the sensor that has the closest intensity value to Mid and define that position as the edge position. In addition, the absorbance change of whole area of the printed gradient-based sensor was calculated.

5.3 Results and Discussion

5.3.1 Array sensitivity

Figure 5.3 shows a quick test of printed gradient-based sensor array at a high concentration of HCHO, O_3 and NO_2, respectively. The result in Figure 5.3 (a) shows that when the sensor chip was exposed to HCHO, only the line of printed HCHO sensor has a response. The color change from yellow to red and the color development is gradually along the gas diffusion direction. In Figure 5.3 (b), only the O_3 sensor changed color from blue to light yellow while both NO_2 and HCHO sensor has a response to high concentration of NO_2. However, the sensor response of HCHO can always be compensated if NO_2 occurred.

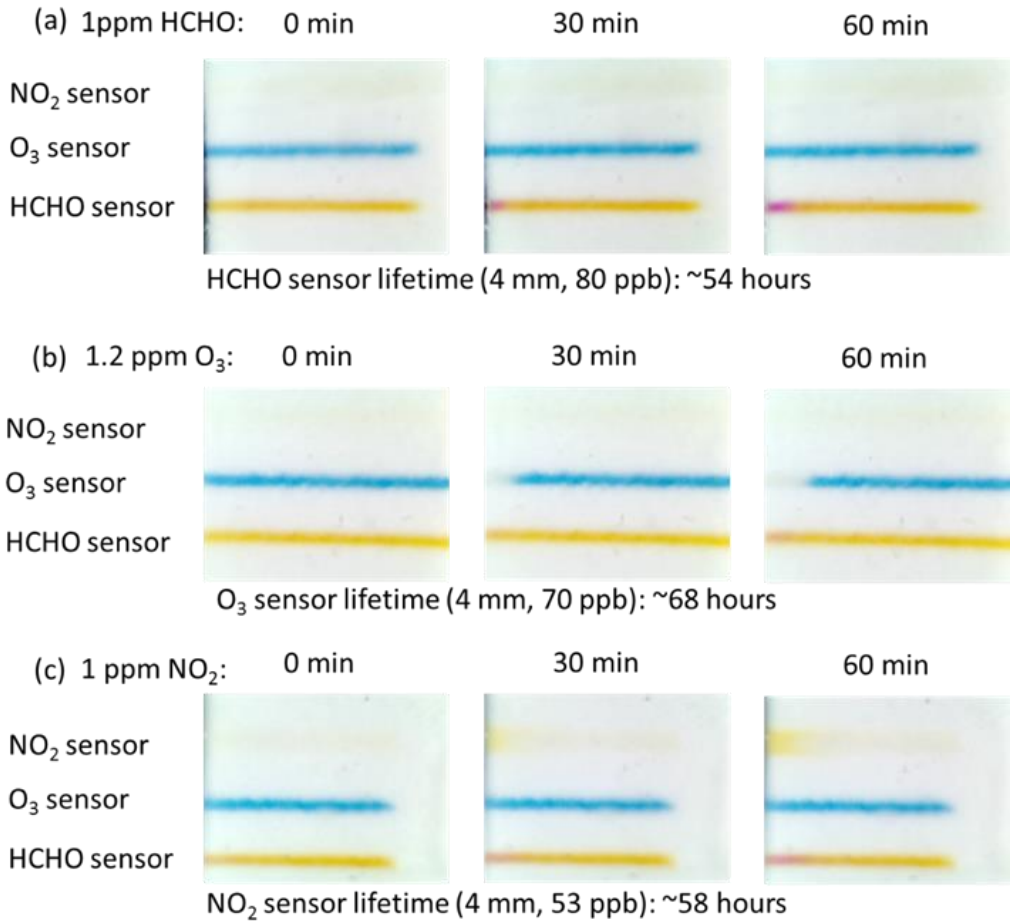

Figure 5.3 Inkjet-printed gradient-based colorimetric sensor arrays tested at high concentration of HCHO, O_3 and NO_2 for an hour, respectively.

5.3.2 Field tests

Figure. 5.6 (b) shows the comparison of ozone reference monitor (2B technology) and ozone sensors reading over 30 hours. Three inkjet-printed ozone sensors were used in this test and the images in Figure 5.6 (a) show the sensor before and after the 30-hour- test. It can be observed that both ozone sensor and reference monitor reflect daily ozone concentration fluctuation.

(a)

Before

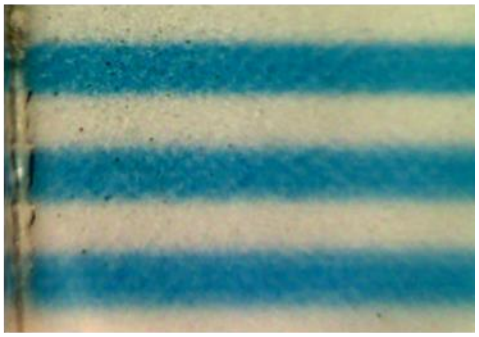

After

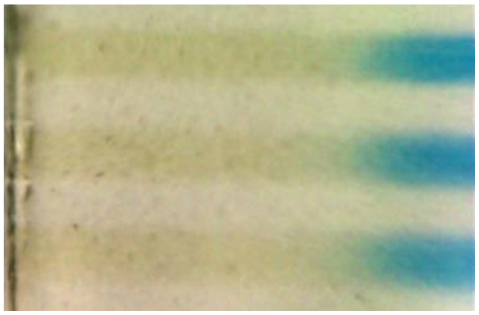

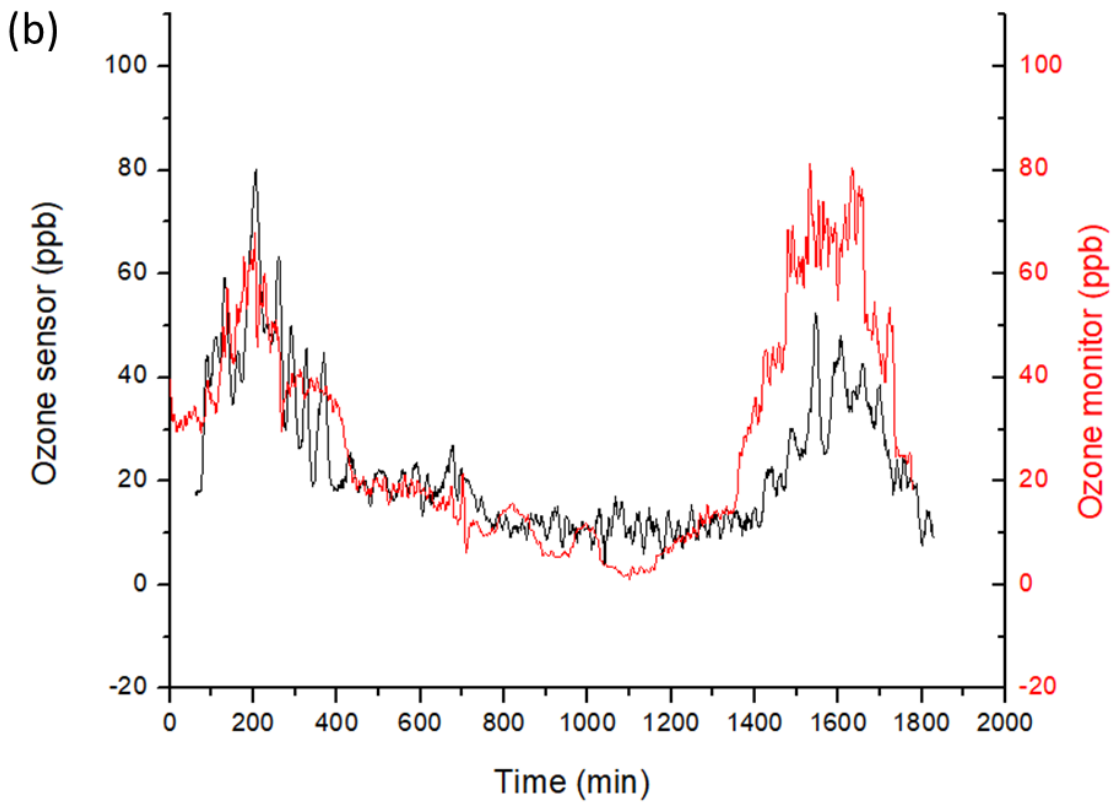

Figure 5.4 Real-time continuous monitoring of ambient ozone concentration, comparison between gradient-based ozone colorimetric sensor and ozone monitor.

5.4 Conclusion

A miniaturized, integrated gradient-based colorimetric array for environmental monitoring has been developed. It demonstrated that different sensing elements for O_3, NO_2, HCHO can be all integrated into the same sensing substrate, making it possible to do real-time multianalyte monitoring, making the device even more attractive since different potential asthma triggers can be simultaneously monitored. The fabrication method using

inkjet printing technology is scalable, cheap, and combined with low-cost hardware, can be deployed in a large scale for clinical and epidemiological studies.

References

[13] *Dräger-Tube/CMS Handbook: Handbook for short term measurements in soil, water and air investigations as well as technical gas analysis.* 16th Edition ed.; Dräger Safety AG & Co KGaA: Lübeck, 2011; p 225.

[26] Guarnieri, M.; Balmes, J. R., Outdoor air pollution and asthma. *The lancet* **2014,** *383* (9928), 1581-1592.

[81] Pattemore, P. K.; Asher, M. I.; Harrison, A. C.; Mitchell, E. A.; Rea, H. H.; Stewart, A. W., The interrelationship among bronchial hyperresponsiveness, the diagnosis of asthma, and asthma symptoms. *Am Rev Respir Dis* **1990,** *142* (3), 549-554.

[82] Herberger, S.; Herold, M.; Ulmer, H.; Burdack-Freitag, A.; Mayer, F., Detection of human effluents by a MOS gas sensor in correlation to VOC quantification by GC/MS. *Building and Environment* **2010,** *45* (11), 2430-2439.

[83] Herberger, S.; Ulmer, H., Indoor air quality monitoring improving air quality perception. *CLEAN–Soil, Air, Water* **2012,** *40* (6), 578-585.

[84] Hotovy, I.; Rehacek, V.; Siciliano, P.; Capone, S.; Spiess, L., Sensing characteristics of NiO thin films as NO_2 gas sensor. *Thin Solid Films* **2002,** *418* (1), 9-15.

[85] Cross, E. S.; Williams, L. R.; Lewis, D. K.; Magoon, G. R.; Onasch, T. B.; Kaminsky, M. L.; Worsnop, D. R.; Jayne, J. T., Use of electrochemical sensors for measurement of air pollution: correcting interference response and validating measurements. *Atmospheric Measurement Techniques* **2017,** *10* (9), 3575-3588.

[86] Tsujita, W.; Kaneko, S.; Ueda, T.; Ishida, H.; Moriizumi, T. In *Sensor-based air-pollution measurement system for environmental monitoring network*, TRANSDUCERS'03. 12th International Conference on Solid-State Sensors, Actuators and Microsystems. Digest of Technical Papers (Cat. No. 03TH8664), IEEE: 2003; pp 544-547.

[87] Cowburn, T.; Cutler, S.; Kelly, M. J., Electrochemical gas sensor. Google Patents: 2010.

[88] Sirringhaus, H.; Kawase, T.; Friend, R. H.; Shimoda, T.; Inbasekaran, M.; Wu, W.; Woo, E. P., High-Resolution Inkjet Printing of All-Polymer Transistor Circuits. *Science* **2000,** *290* (5499), 2123-2126.

[89] Sele, C. W.; von Werne, T.; Friend, R. H.; Sirringhaus, H., Lithography-Free, Self-Aligned Inkjet Printing with Sub-Hundred-Nanometer Resolution. *Advanced Materials* **2005,** *17* (8), 997-1001.

[90] De Gans, B.-J.; Duineveld, P. C.; Schubert, U. S., Inkjet Printing of Polymers: State of the Art and Future Developments. *Advanced Materials* **2004,** *16* (3), 203-213.

6 CONCLUSION AND FUTURE WORK

Three generations of novel colorimetric sensors have been developed. The first generation is mosaic colorimetric sensor based on tiny sensor blocks and by detecting absorbance change after each air sample injection, the target analyte concentration can be measured. The second generation is a gradient-based colorimetric sensor. Lateral transport of analytes across the colorimetric sensor surface creates a color gradient that shifts along the transport direction over time, and the sensor tracks the gradient shift and converts it into analyte concentration in real-time. The third generation is gradient-based colorimetric arrays fabricated by inkjet-printing method that integrates multiple sensors on a miniaturized sensor chip. The presented three generations of colorimetric sensors demonstrated the ability to continuously monitor multiple air pollutants and the sensor lifetime and fabrication methods have been improved over each generation. Ozone, nitrogen dioxide, formaldehyde and carbon monoxide are chosen as analytes of interest. The performance of sensors has been validated in the lab and field tests, proving the capability of the sensors to be used for personal exposure monitoring.

One direction for future work is to keep adding more gas analytes to the detecting list. The more gas analytes could be detected, the more information could be gathered. Also, a humidity sensor could be added on the sensor chip so the humidity level on the sensor can be detected.

Another possibility is to take advantage of the rapidly growing cloud computing technology. One possible disadvantage of adding more gas analytes to a device for detection is that the data processing would be much slower. Therefore, one way to solve

this problem is to share all the test results. For example, if a device can detect NO_2 and HCHO, and another device nearby can detect O_3 and CO, and those devices could share the results with each other through the cloud and both can get data of four pollutants. A map of contaminant levels can be drawn from all other devices there without having to travel to that area.

REFERENCES

[1] Bernstein, J. A.; Alexis, N.; Bacchus, H.; Bernstein, I. L.; Fritz, P.; Horner, E.; Li, N.; Mason, S.; Nel, A.; Oullette, J., The health effects of nonindustrial indoor air pollution. *Journal of Allergy and Clinical Immunology* **2008,** *121* (3), 585-591.

[2] Samet, J. M.; Marbury, M. C.; Spengler, J. D., Health effects and sources of indoor air pollution. Part I. *American Review of Respiratory Disease* **1987,** *136* (6), 1486-1508.

[3] Schwartz, J., Air pollution and hospital admissions for heart disease in eight US counties. *Epidemiology* **1999**, 17-22.

[4] Cohen, A. J., Outdoor air pollution and lung cancer. *Environmental health perspectives* **2000,** *108* (suppl 4), 743-750.

[5] Hwang, J.-S.; Chan, C.-C., Effects of air pollution on daily clinic visits for lower respiratory tract illness. *American journal of epidemiology* **2002,** *155* (1), 1-10.

[6] National Ambient Air Quality Standards. https://www.epa.gov/criteria-air-pollutants/naaqs-table#3.

[7] WHO, Air quality guidelines for Europe. **2000**.

[8] Occupational Safety and Health Standards-Formaldehyde. https://www.osha.gov/pls/oshaweb/owadisp.show_document?p_id=10075&p_table=STANDARDS.

[9] Wennrich, L.; Popp, P.; Hafner, C., Novel integrative passive samplers for the long-term monitoring of semivolatile organic air pollutants. *Journal of Environmental Monitoring* **2002,** *4* (3), 371-376.

[10] Klánová, J.; Kohoutek, J.; Hamplová, L.; Urbanová, P.; Holoubek, I., Passive air sampler as a tool for long-term air pollution monitoring: Part 1. Performance assessment for seasonal and spatial variations. *Environmental Pollution* **2006,** *144* (2), 393-405.

[11] Zhao, B.; Zhang, S.; Zhou, Y.; He, D.; Li, Y.; Ren, M.; Xu, Z.; Fang, J., Characterization and quantification of PAH atmospheric pollution from a large petrochemical complex in Guangzhou: GC–MS/MS analysis. *Microchemical journal* **2015,** *119*, 140-144.

[12] Gilchrist, A.; Nobbs, J., Colorimetry, Theory. In *Encyclopedia of Spectroscopy and Spectrometry*, Lindon, J. C., Ed. Elsevier: Oxford, 1999; pp 337-343.

[13] *Dräger-Tube/CMS Handbook: Handbook for short term measurements in soil, water and air investigations as well as technical gas analysis.* 16th Edition ed.; Dräger Safety AG & Co KGaA: Lübeck, 2011; p 225.

[14] Feng, L.; Musto, C. J.; Kemling, J. W.; Lim, S. H.; Suslick, K. S., A colorimetric sensor array for identification of toxic gases below permissible exposure limits. *Chemical Communications* **2010,** *46* (12), 2037-2039.

[15] Lim, S. H.; Feng, L.; Kemling, J. W.; Musto, C. J.; Suslick, K. S., An optoelectronic nose for the detection of toxic gases. *Nature chemistry* **2009,** *1* (7), 562.

[16] Huang, X.-w.; Zou, X.-b.; Shi, J.-y.; Guo, Y.; Zhao, J.-w.; Zhang, J.; Hao, L., Determination of pork spoilage by colorimetric gas sensor array based on natural pigments. *Food chemistry* **2014,** *145*, 549-554.

[17] Brunekreef, B.; Holgate, S. T., Air pollution and health. *The lancet* **2002,** *360* (9341), 1233-1242.

[18] Mills, N. L.; Donaldson, K.; Hadoke, P. W.; Boon, N. A.; MacNee, W.; Cassee, F. R.; Sandström, T.; Blomberg, A.; Newby, D. E., Adverse cardiovascular effects of air pollution. *Nature clinical practice Cardiovascular medicine* **2009,** *6* (1), 36-44.

[19] Saxon, A.; Diaz-Sanchez, D., Air pollution and allergy: you are what you breathe. *Nature immunology* **2005,** *6* (3), 223-226.

[20] Smith, K. R.; Samet, J. M.; Romieu, I.; Bruce, N., Indoor air pollution in developing countries and acute lower respiratory infections in children. *Thorax* **2000,** *55* (6), 518-532.

[21] Morris, R. D.; Naumova, E. N.; Munasinghe, R. L., Ambient air pollution and hospitalization for congestive heart failure among elderly people in seven large US cities. *American journal of public health* **1995,** *85* (10), 1361-1365.

[22] Simoni, M.; Jaakkola, M.; Carrozzi, L.; Baldacci, S.; Di Pede, F.; Viegi, G., Indoor air pollution and respiratory health in the elderly. *European Respiratory Journal* **2003,** *21* (40 suppl), 15s-20s.

[23] Kim, J. J., Ambient air pollution: health hazards to children. *Pediatrics* **2004,** *114* (6), 1699-1707.

[24] Ruckerl, R.; Ibald-Mulli, A.; Koenig, W.; Schneider, A.; Woelke, G.; Cyrys, J.; Heinrich, J.; Marder, V.; Frampton, M.; Wichmann, H. E., Air pollution and markers of inflammation and coagulation in patients with coronary heart disease.

American journal of respiratory and critical care medicine **2006,** *173* (4), 432-441.

[25] Jerrett , M.; Burnett , R. T.; Pope , C. A. I.; Ito , K.; Thurston , G.; Krewski , D.; Shi , Y.; Calle , E.; Thun , M., Long-Term Ozone Exposure and Mortality. *New England Journal of Medicine* **2009,** *360* (11), 1085-1095.

[26] Guarnieri, M.; Balmes, J. R., Outdoor air pollution and asthma. *The lancet* **2014,** *383* (9928), 1581-1592.

[27] Lelieveld, J.; Evans, J. S.; Fnais, M.; Giannadaki, D.; Pozzer, A., The contribution of outdoor air pollution sources to premature mortality on a global scale. *Nature* **2015,** *525* (7569), 367-371.

[28] Brauer, M.; Hoek, G.; Smit, H.; De Jongste, J.; Gerritsen, J.; Postma, D. S.; Kerkhof, M.; Brunekreef, B., Air pollution and development of asthma, allergy and infections in a birth cohort. *European Respiratory Journal* **2007,** *29* (5), 879-888.

[29] Stieb, D. M.; Chen, L.; Eshoul, M.; Judek, S., Ambient air pollution, birth weight and preterm birth: a systematic review and meta-analysis. *Environmental research* **2012,** *117*, 100-111.

[30] Wilson, E., EPIDEMIOLOGY Long-term exposure to ozone increases risk of death. *Chemical & Engineering News Archive* **2009,** *87* (11), 9.

[31] Pope III, C. A.; Burnett, R. T.; Thun, M. J.; Calle, E. E.; Krewski, D.; Ito, K.; Thurston, G. D., Lung cancer, cardiopulmonary mortality, and long-term exposure to fine particulate air pollution. *Jama* **2002,** *287* (9), 1132-1141.

[32] Patocka, J.; Kuca, K., Irritant compounds: respiratory irritant gases. *Milit Med Sci Lett* **2014,** *83* (2), 73-82.

[33] Torres-Jardon, R.; Keener, T. C., Evaluation of ozone-nitrogen oxides-volatile organic compound sensitivity of Cincinnati, Ohio. *Journal of the Air & Waste Management Association* **2006,** *56* (3), 322-333.

[34] Shah, A. S.; Lee, K. K.; McAllister, D. A.; Hunter, A.; Nair, H.; Whiteley, W.; Langrish, J. P.; Newby, D. E.; Mills, N. L., Short term exposure to air pollution and stroke: systematic review and meta-analysis. *bmj* **2015,** *350*, h1295.

[35] Lin, S.; Liu, X.; Le, L. H.; Hwang, S.-A., Chronic exposure to ambient ozone and asthma hospital admissions among children. *Environmental health perspectives* **2008,** *116* (12), 1725-1730.

[36] McConnell, R.; Berhane, K.; Gilliland, F.; London, S. J.; Islam, T.; Gauderman, W. J.; Avol, E.; Margolis, H. G.; Peters, J. M., Asthma in exercising children exposed to ozone: a cohort study. *The lancet* **2002,** *359* (9304), 386-391.

[37] Khaniabadi, Y. O.; Hopke, P. K.; Goudarzi, G.; Daryanoosh, S. M.; Jourvand, M.; Basiri, H., Cardiopulmonary mortality and COPD attributed to ambient ozone. *Environmental research* **2017,** *152*, 336-341.

[38] Sunyer, J.; Jarvis, D.; Gotschi, T.; Garcia-Esteban, R.; Jacquemin, B.; Aguilera, I.; Ackerman, U.; de Marco, R.; Forsberg, B.; Gislason, T., Chronic bronchitis and urban air pollution in an international study. *Occupational and environmental medicine* **2006,** *63* (12), 836-843.

[39] Latza, U.; Gerdes, S.; Baur, X., Effects of nitrogen dioxide on human health: systematic review of experimental and epidemiological studies conducted between 2002 and 2006. *International journal of hygiene and environmental health* **2009,** *212* (3), 271-287.

[40] BLOMBERG, A.; Krishna, M. T.; Bocchino, V.; Biscione, G. L.; Shute, J. K.; Kelly, F. J.; Frew, A. J.; Holgate, S. T.; Sandstrom, T., The inflammatory effects of 2 ppm NO_2 on the airways of healthy subjects. *American journal of respiratory and critical care medicine* **1997,** *156* (2), 418-424.

[41] Barck, C.; Sandström, T.; Lundahl, J.; Hallden, G.; Svartengren, M.; Strand, V.; Rak, S.; Bylin, G., Ambient level of NO_2 augments the inflammatory response to inhaled allergen in asthmatics. *Respiratory medicine* **2002,** *96* (11), 907-917.

[42] Chauhan, A.; Inskip, H. M.; Linaker, C. H.; Smith, S.; Schreiber, J.; Johnston, S. L.; Holgate, S. T., Personal exposure to nitrogen dioxide (NO_2) and the severity of virus-induced asthma in children. *The lancet* **2003,** *361* (9373), 1939-1944.

[43] PERSHAGEN, G.; Rylander, E.; Norberg, S.; Eriksson, M.; Nordvall, S. L., Air pollution involving nitrogen dioxide exposure and wheezing bronchitis in children. *International journal of epidemiology* **1995,** *24* (6), 1147-1153.

[44] MEYER, B.; HERMANNS, K., Formaldehyde release from pressed wood products. ACS Publications: 1985.

[45] Kelly, T. J.; Smith, D. L.; Satola, J., Emission rates of formaldehyde from materials and consumer products found in California homes. *Environmental Science & Technology* **1999,** *33* (1), 81-88.

[46] Fowler, J. F.; Skinner, S. M.; Belsito, D. V., Allergic contact dermatitis from formaldehyde resins in permanent press clothing: an underdiagnosed cause of generalized dermatitis. *Journal of the American Academy of Dermatology* **1992,** *27* (6), 962-968.

[47] Conner, A. H., Urea-formaldehyde adhesive resins. *Polymeric materials encyclopedia* **1996,** *11*, 8496-8501.

[48] Kim, K.-H.; Jahan, S. A.; Lee, J.-T., Exposure to formaldehyde and its potential human health hazards. *Journal of Environmental Science and Health, Part C* **2011,** *29* (4), 277-299.

[49] Krzyzanowski, M.; Quackenboss, J. J.; Lebowitz, M. D., Chronic respiratory effects of indoor formaldehyde exposure. *Environmental research* **1990,** *52* (2), 117-125.

[50] Bosetti, C.; McLaughlin, J.; Tarone, R.; Pira, E.; La Vecchia, C., Formaldehyde and cancer risk: a quantitative review of cohort studies through 2006. *Annals of Oncology* **2008,** *19* (1), 29-43.

[51] McGwin, G.; Lienert, J.; Kennedy, J. I., Formaldehyde Exposure and Asthma in Children: A Systematic Review. *Environmental health perspectives* **2010,** *118* (3), 313-317.

[52] Blair, A.; Saracci, R.; Stewart, P. A.; Hayes, R. B.; Shy, C., Epidemiologic evidence on the relationship between formaldehyde exposure and cancer. *Scandinavian Journal of Work, Environment & Health* **1990,** *16* (6), 381-393.

[53] Rajiah, K.; Mathew, E. M., Clinical manifestation, effects, diagnosis, monitoring of carbon monoxide poisoning and toxicity. *Afr. J. Pharm. Pharmacol.* **2011,** *5* (2), 259-63.

[54] Raub, J. A.; Mathieu-Nolf, M.; Hampson, N. B.; Thom, S. R., Carbon monoxide poisoning—a public health perspective. *Toxicology* **2000,** *145* (1), 1-14.

[55] Types of air pollution. https://cceeb.org/resources/air-quality-101/#toxic-air-contaminants.

[56] Sampling Methods for Criteria Pollutants. https://aqs.epa.gov/aqsweb/documents/codetables/methods_criteria.html.

[57] Toby, S., Chemiluminescence in the reactions of ozone. *Chemical Reviews* **1984,** *84* (3), 277-285.

[58] Andersen, P. C.; Williford, C. J.; Birks, J. W., Miniature Personal Ozone Monitor Based on UV Absorbance. *Analytical Chemistry* **2010,** *82* (19), 7924-7928.

[59] Zhao, D. A Novel Handheld Real-time Carbon Dioxide Analyzer for Health and Environmental Applications Arizona State University, 2014.

[60] Badjagbo, K.; Sauvé, S.; Moore, S., Real-time continuous monitoring methods for airborne VOCs. *TrAC Trends in Analytical Chemistry* **2007,** *26* (9), 931-940.

[61] Cao, T.; Thompson, J. E., Personal monitoring of ozone exposure: A fully portable device for under $150 USD cost. *Sensors and Actuators B: Chemical* **2016,** *224*, 936-943.

[62] Shafiei, M.; Kalantar-Zadeh, K.; Wlodarski, W.; Comini, E.; Ferroni, M.; Sberveglieri, G.; Kaciulis, S.; Pandolfi, L., Hydrogen gas sensing performance of Pt/SnO_2 nanowires/SiC MOS devices. *Int. J. Smart Sens. Intell. Syst* **2008,** *1* (3), 771.

[63] MOS type sensors operating principle. http://www.figarosensor.com/technicalinfo/principle/mos-type.html.

[64] Electrochemical type sensors operating principle. http://www.figarosensor.com/technicalinfo/principle/electrochemical-type.html.

[65] Dominici, F.; Peng, R. D.; Barr, C. D.; Bell, M. L., Protecting human health from air pollution: shifting from a single-pollutant to a multipollutant approach. *Epidemiology (Cambridge, Mass.)* **2010,** *21* (2), 187-194.

[66] Dons, E.; Laeremans, M.; Orjuela, J. P.; Avila-Palencia, I.; Carrasco-Turigas, G.; Cole-Hunter, T.; Anaya-Boig, E.; Standaert, A.; De Boever, P.; Nawrot, T.; Götschi, T.; de Nazelle, A.; Nieuwenhuijsen, M.; Int Panis, L., Wearable Sensors for Personal Monitoring and Estimation of Inhaled Traffic-Related Air Pollution: Evaluation of Methods. *Environmental Science & Technology* **2017,** *51* (3), 1859-1867.

[67] Hu, K.; Davison, T.; Rahman, A.; Sivaraman, V., Air Pollution Exposure Estimation and Finding Association with Human Activity using Wearable Sensor Network. In *Proceedings of the MLSDA 2014 2nd Workshop on Machine Learning for Sensory Data Analysis*, ACM: Gold Coast, Australia QLD, Australia, 2014; pp 48-55.

[68] Tsow, F.; Forzani, E.; Rai, A.; Wang, R.; Tsui, R.; Mastroianni, S.; Knobbe, C.; Gandolfi, A. J.; Tao, N. J., A Wearable and Wireless Sensor System for Real-Time Monitoring of Toxic Environmental Volatile Organic Compounds. *IEEE Sensors Journal* **2009,** *9* (12), 1734-1740.

[69] Rai, P.; Kim, Y.-S.; Song, H.-M.; Song, M.-K.; Yu, Y.-T., The role of gold catalyst on the sensing behavior of ZnO nanorods for CO and NO_2 gases. *Sens. Actuators, B* **2012,** *165* (1), 133-142.

[70] Yanagimoto, T.; Yu, Y. T.; Kaneko, K., Microstructure and CO gas sensing property of Au/SnO_2 core–shell structure nanoparticles synthesized by

precipitation method and microwave-assisted hydrothermal synthesis method. *Sens. Actuators, B* **2012,** *166–167*, 31-35.

[71] Lewis, A.; Edwards, P., Validate personal air-pollution sensors. *Nature* **2016,** *535* (7610), 29-31.

[72] Wetchakun, K.; Samerjai, T.; Tamaekong, N.; Liewhiran, C.; Siriwong, C.; Kruefu, V.; Wisitsoraat, A.; Tuantranont, A.; Phanichphant, S., Semiconducting metal oxides as sensors for environmentally hazardous gases. *Sensors and Actuators B: Chemical* **2011,** *160* (1), 580-591.

[73] Li, J.; Lu, Y.; Ye, Q.; Cinke, M.; Han, J.; Meyyappan, M., Carbon Nanotube Sensors for Gas and Organic Vapor Detection. *Nano Letters* **2003,** *3* (7), 929-933.

[74] Vallejos, S.; Khatko, V.; Aguir, K.; Ngo, K. A.; Calderer, J.; Gràcia, I.; Cané, C.; Llobet, E.; Correig, X., Ozone monitoring by micro-machined sensors with WO_3 sensing films. *Sensors and Actuators B: Chemical* **2007,** *126* (2), 573-578.

[75] Kamionka, M.; Breuil, P.; Pijolat, C., Calibration of a multivariate gas sensing device for atmospheric pollution measurement. *Sensors and Actuators B: Chemical* **2006,** *118* (1), 323-327.

[76] Koutrakis, P.; Wolfson, J. M.; Bunyaviroch, A.; Froehlich, S. E.; Hirano, K.; Mulik, J. D., Measurement of ambient ozone using a nitrite-coated filter. *Analytical Chemistry* **1993,** *65* (3), 209-214.

[77] Peterson, P.; Aujla, A.; Grant, K.; Brundle, A.; Thompson, M.; Vande Hey, J.; Leigh, R., Practical Use of Metal Oxide Semiconductor Gas Sensors for Measuring Nitrogen Dioxide and Ozone in Urban Environments. *Sensors* **2017,** *17* (7), 1653.

[78] Lin, C.; Xian, X.; Qin, X.; Wang, D.; Tsow, F.; Forzani, E.; Tao, N., High Performance Colorimetric Carbon Monoxide Sensor for Continuous Personal Exposure Monitoring. *ACS Sensors* **2018,** *3* (2), 327-333.

[79] Lewis, A. C.; Lee, J. D.; Edwards, P. M.; Shaw, M. D.; Evans, M. J.; Moller, S. J.; Smith, K. R.; Buckley, J. W.; Ellis, M.; Gillot, S. R.; White, A., Evaluating the performance of low cost chemical sensors for air pollution research. *Faraday Discussions* **2016,** *189* (0), 85-103.

[80] Bernstein, M.; Whitman, D., The Challenges of Battling Ozone Pollution. *Environment: Science and Policy for Sustainable Development* **2005,** *47* (8), 28-41.

[81] Pattemore, P. K.; Asher, M. I.; Harrison, A. C.; Mitchell, E. A.; Rea, H. H.; Stewart, A. W., The interrelationship among bronchial hyperresponsiveness, the

diagnosis of asthma, and asthma symptoms. *Am Rev Respir Dis* **1990,** *142* (3), 549-554.

[82] Herberger, S.; Herold, M.; Ulmer, H.; Burdack-Freitag, A.; Mayer, F., Detection of human effluents by a MOS gas sensor in correlation to VOC quantification by GC/MS. *Building and Environment* **2010,** *45* (11), 2430-2439.

[83] Herberger, S.; Ulmer, H., Indoor air quality monitoring improving air quality perception. *CLEAN–Soil, Air, Water* **2012,** *40* (6), 578-585.

[84] Hotovy, I.; Rehacek, V.; Siciliano, P.; Capone, S.; Spiess, L., Sensing characteristics of NiO thin films as NO_2 gas sensor. *Thin Solid Films* **2002,** *418* (1), 9-15.

[85] Cross, E. S.; Williams, L. R.; Lewis, D. K.; Magoon, G. R.; Onasch, T. B.; Kaminsky, M. L.; Worsnop, D. R.; Jayne, J. T., Use of electrochemical sensors for measurement of air pollution: correcting interference response and validating measurements. *Atmospheric Measurement Techniques* **2017,** *10* (9), 3575-3588.

[86] Tsujita, W.; Kaneko, S.; Ueda, T.; Ishida, H.; Moriizumi, T. In *Sensor-based air-pollution measurement system for environmental monitoring network*, TRANSDUCERS'03. 12th International Conference on Solid-State Sensors, Actuators and Microsystems. Digest of Technical Papers (Cat. No. 03TH8664), IEEE: 2003; pp 544-547.

[87] Cowburn, T.; Cutler, S.; Kelly, M. J., Electrochemical gas sensor. Google Patents: 2010.

[88] Sirringhaus, H.; Kawase, T.; Friend, R. H.; Shimoda, T.; Inbasekaran, M.; Wu, W.; Woo, E. P., High-Resolution Inkjet Printing of All-Polymer Transistor Circuits. *Science* **2000,** *290* (5499), 2123-2126.

[89] Sele, C. W.; von Werne, T.; Friend, R. H.; Sirringhaus, H., Lithography-Free, Self-Aligned Inkjet Printing with Sub-Hundred-Nanometer Resolution. *Advanced Materials* **2005,** *17* (8), 997-1001.

[90] de Gans, B.-J.; Duineveld, P. C.; Schubert, U. S., Inkjet Printing of Polymers: State of the Art and Future Developments. *Advanced Materials* **2004,** *16* (3), 203-213.